NATIONAL ADVISORY COMMITTEE FOR AERONAUTICS

TECHNICAL NOTE 2936

COMBUSTION INSTABILITY IN AN ACID-HEPTANE ROCKET WITH A PRESSURIZED-GAS PROPELLANT PUMPING SYSTEM

By Adelbert O. Tischler and Donald R. Bellman

Lewis Flight Propulsion Laboratory
Cleveland, Ohio

Washington
May 1953

NATIONAL ADVISORY COMMITTEE FOR AERONAUTICS

TECHNICAL NOTE 2936

COMBUSTION INSTABILITY IN AN ACID-HEPTANE ROCKET WITH A PRESSURIZED-GAS PROPELLANT PUMPING SYSTEM

By Adelbert O. Tischler and Donald R. Bellman

SUMMARY

Results of experimental measurements of low-frequency combustion instability of a 300-pound-thrust acid-heptane rocket engine were compared with the trends predicted by an analysis of combustion instability in a rocket engine with a pressurized-gas propellant pumping system. The simplified analysis, which assumes a monopropellant model, was based on the concept that a combustion time delay occurred from the moment of propellant injection to the moment of propellant combustion. This combustion time delay was experimentally measured; the experimental values were approximately half the magnitude predicted by the analysis. The pressure-fluctuation frequency for a rocket engine with a characteristic length of 100 inches operated at a combustion-chamber pressure of 280 pounds per square inch absolute was 38 cycles per second; the analysis indicated a frequency of 37 cycles per second. Increasing combustion-chamber characteristic length decreased the pressure-fluctuation frequency, in conformity with the analysis. Increasing the chamber operating pressure or increasing the injector pressure drop increased the frequency. These latter two effects are contrary to the analysis; the discrepancies are attributed to the conflict between the assumptions made to simplify the analysis and the experimental conditions. Oxidant-fuel ratio had no apparent effect on the experimentally measured pressure-fluctuation frequency for acid-heptane ratios from 3.0 to 7.0. The frequencies decreased with increased amplitude of the combustion-chamber pressure variations. The analysis indicated that if the combustion time delay were sufficiently short, low-frequency combustion instability would be eliminated.

INTRODUCTION

Development of rocket engines for flight propulsion has disclosed combustion instabilities which often result in destruction of the rocket engine by stress failure or burnout of the combustion chamber. A cyclical low-frequency type of instability which exhibits chamber pressure and nozzle flow or thrust fluctuations in the frequency range from 10 to 200 cycles per second is called chugging. This type of instability may reduce

specific impulse and is believed to be accompanied by changes in combustion efficiency. High-speed photographs of this type of instability are shown in reference 1. A higher-frequency mode of instability, which manifests itself in greatly increased heat-transfer rates in the rocket combustion chamber and which generally results in chamber burnouts, is called screaming. Whether these combustion instabilities are distinctly separate or are related phenomena in different frequency ranges has not been definitely established, because the origin and nature of the instabilities are unknown.

It has been postulated that chugging is a result of out-of-phase coupling between the combustion-chamber pressure and the fluid flow in the propellant feed system. Analyses of the chugging phenomenon in a rocket engine with a pressurized-gas propellant pumping system have been made on this basis. The significance of the ratio of feed-line pressure drop to the absolute chamber pressure in determining whether chugging can occur is discussed in reference 2. The stability range of operation of a rocket engine is further defined in reference 3. This analysis derived the following expression as a limit of stable rocket operation:

$$\frac{(\Delta p)_{cr}}{p_c} = \frac{1}{2\sqrt{1 + \left(\frac{t_c}{t_o}\right)^2}}$$

where

$(\Delta p)_{cr}$ critical pressure drop in propellant feed system at which chugging can occur

p_c absolute rocket combustion-chamber pressure

t_c combustion-chamber time constant equal to twice characteristic length divided by characteristic exhaust velocity

t_o period of oscillations, sec/radian

The accelerations of fluid masses in the propellant feed lines during transients were neglected.

Early analyses of chugging did not readily show the effects on the chugging characteristics of a rocket engine of varying the rocket design and operating parameters. In order to gain insight into the effects of rocket design and operating parameters on chugging characteristics, a brief series of experiments with a 300-pound thrust acid-heptane rocket

with a pressurized-gas propellant pumping system was conducted at the NACA Lewis laboratory. In addition, a simplified analysis was made of the chugging instability of a monopropellant rocket engine. This analysis, completed in 1949, was based on the premise that chugging is caused by an out-of-phase coupling between the fluid flow of the propellant feed system and the combustion process in the rocket chamber. The experimental results of varying operating and design parameters were compared with the trends predicted by the analysis. The time delay between propellant injection and combustion, which was postulated in the analytical development, was experimentally measured; and the effects of varying chamber characteristic length, rocket combustion-chamber pressure, injection velocity, and oxidant-fuel ratio on the chugging frequencies were experimentally investigated. The results of the experimental investigation are compared with the analytically predicted trends. The derivation of the analysis and the trends predicted by it for a typical rocket engine are presented in appendix A.

ANALYSIS OF LOW-FREQUENCY COMBUSTION VIBRATIONS

The analysis is based on the concept of an out-of-phase coupling between the propellant flow and the rocket combustion-chamber pressure. This concept can be illustrated by considering the simplified monopropellant rocket engine shown in figure 1. A pressurized gas is used to pump the liquid monopropellant. Under steady-flow conditions the combustion-chamber pressure is established by the gas pressure in the propellant tank, the pressure drop in the propellant feed system and that across the injector orifices, and the pressure drop across the rocket exhaust nozzle. If the combustion-chamber pressure is momentarily lowered an increase in propellant flow will occur which will tend to re-establish equilibrium conditions. The rise in propellant flow, however, will not occur simultaneously with the drop of chamber pressure because of inertia of the fluid in the propellant feed line. This delay is hereinafter called the inertia time lag. The delayed propellant-flow increase results in an increased combustion rate after a second significant time delay due to injection, impingement, mixing, vaporizing, preignition reactions, ignition, and combustion. This second time delay is called the combustion time delay. Because of the necessity of charging the chamber volume with gas, the increased combustion rate results in corresponding increased pressure only after a third time delay, which will be called the charging time lag. During these time delays, an excess of propellant enters the chamber. Therefore, when the pressure does rise it exceeds the value necessary to restore equilibrium operating conditions. The high pressure eventually causes the propellant flow to drop below normal, with a subsequent lowering of chamber pressure. Thus in the absence of sufficient damping a cycling condition of propellant flow and combustion-chamber pressure can become established.

The analysis yields an expression of the following form (all symbols are defined in appendix B):

$$A\frac{d^2f(t)}{dt^2} + B\frac{df(t)}{dt} + Cf(t) + f(t - \theta) = 0$$

The solution of this expression for stable chugging operation can be found in two simultaneous equations:

$$-A\omega^2 + C + \cos \omega\theta = 0$$

$$B\omega - \sin \omega\theta = 0$$

The two simultaneous equations yield unique solutions for the combustion time delay θ and the cycling frequency ω in terms of the constants A, B, and C, which are dependent on the rocket-engine configuration and operating conditions. The values of θ and ω represent the minimum combustion time delay which will permit the rocket engine to sustain chugging and the corresponding maximum chugging frequency; that is, these solutions represent the condition at which the amplitude of the chugging oscillations will be neither amplified nor damped. Chugging with longer combustion time delays at lower cycling frequencies is possible, but in this case the chugging amplitude theoretically will increase with each cycle, and the equations of the analysis will no longer apply. If the combustion time delay is less than the critical value, any disturbance in the pressure or flow will be damped and will soon die out.

The analytical equations describe a "feedback" loop circuit. Because the combustion time delay was assumed constant, the "gain" or amplification of the loop is accomplished by a proper phase relation between flow and pressure change. Amplification or gain by other processes is not considered.

The analysis does not provide means for predicting experimental combustion time delays; its value lies in the determination of the critical combustion time delay which will permit chugging and the indication of the probable effects on the critical combustion time delay of changing rocket design and operating parameters.

Complete derivation of the analytical equations, the assumptions on which the analysis is based, and the chugging trends predicted for an acid-heptane rocket for a typical range of rocket design and operating conditions are given in appendix A.

EXPERIMENTAL INVESTIGATION OF COMBUSTION INSTABILITY

Apparatus and Instrumentation

The rocket engine used for the experimental investigation of chugging was a 300-pound thrust uncooled rocket with white fuming nitric acid and commercial n-heptane as propellants. Two rocket chambers were

used; one with a characteristic length of 100 inches and the other with a characteristic length of 200 inches. The internal diameter of each chamber was four inches. The injector comprised four pairs of heptane-on-acid impinging-type jets. Several sets of orifices of different diameters with acid and fuel orifices matched so as to maintain an approximately equal ratio of acid injector orifice area to heptane orifice area were employed.

The rocket installation, which is shown diagrammatically in figure 2, used high-pressure helium to pump the acid and heptane to the rocket chamber. Ignition was accomplished by filling the heptane feed line with furfuryl alcohol before firing.

Instrumentation included an electromagnetic induction flowmeter capable of following flow surges up to about 100 surges per second (ref. 4). This meter was installed in the acid feed line about two feet from the rocket engine. Combustion-chamber pressure was detected by a variable-capacitance type diaphragm pressure detector, which was flush-mounted in the chamber wall. The outputs of these instruments, neither of which has any appreciable inherent signal lag, were fed to two oscilloscopes and recorded simultaneously on a moving-film camera. These films provided a time-sequence record of the instantaneous acid propellant flow and the instantaneous combustion-chamber pressure as well as a record of the duration of each pressure and flow pulse (chugging frequency).

Pressure taps at both propellant tanks, just upstream of the injection orifices, and in the combustion chambers were led to Bourdon tube recording pressure gages. Thrust was detected by a strain-gage pickup and recorded by a self-balancing potentiometer.

Propellant consumption was estimated from weights of the propellants before and after each run. The duration of experimental test runs was from 10 to 15 seconds.

Procedure

A series of experimental test runs was made with each of the two rocket-engine chambers. In one series of runs the combustion-chamber pressure was varied by adjusting the propellant-tank pressures. For each rocket engine configuration, chugging runs at several oxidant-fuel ratios were made by adjusting the pressure-setting on the heptane tank.

RESULTS AND DISCUSSION

The rocket-engine instrumentation permitted the experimental measurement of the time lag during chugging between the change of propellant (acid) flow and change of combustion-chamber pressure, as well as the

chugging frequencies and the mean tank, injector, and chamber pressures. A typical flowmeter and pressure trace is shown in figure 3. The flow rate of the acid is proportional to the amplitude of a 400-cycle carrier wave. The chamber-pressure variation is indicated directly by the lower trace. The relations between change of flow and change of pressure are in accordance with the postulated concept that a time interval exists between propellant injection and combustion. A study of the data at starting of a run where a time datum for the flow and pressure traces was available indicated that each change of pressure corresponded to the immediately preceding change of flow; that is, there were no multiple-phase relations between flow and pressure in the experimental chugging runs. Because of diffuculties experienced in the maintenance of the electromagnetic flowmeter the major part of the experimental data is presented in terms of the more easily determined chugging frequency.

Chugging frequency. - The chugging frequency during the course of a typical chugging run is plotted in figure 4. Data points corresponding to each of the first three chugging cycles and then to an average of each succeeding five cycles are shown. The first few chugging waves at the start of a run were of low frequency and considerable pressure amplitude. The waves rapidly increased in frequency during the first one-half second, then decreased somewhat during the following second to a sustained frequency which increased progressively by about 5 percent during the run. At the end of the run, apparently after the propellant valves had begun to close, the chugging frequency again increased.

Other runs showed a similar pattern of chugging frequency during an experimental run. The low-frequency, high-amplitude starting pulses were present in all runs, whether or not sustained chugging occurred. When chugging began after a period of nonchugging operation, a pressure variation of small amplitude and irregular frequency approximately twice the chugging frequency was perceptible in the pressure trace just before chugging began. This pressure variation dropped in frequency to the sustained or "normal" chugging frequency with a great increase in amplitude at the onset of chugging. Sustained chugging of low amplitude never occurred. The chugging frequency about halfway through the sustained chugging part of the run was arbitrarily chosen as the "normal" chugging frequency and this is the chugging frequency used in further plots of the data.

A number of experimental runs began with no apparent rocket chugging, then broke into chugging. A comparison of recorded Bourdon gage pressures and thrust measurements of these runs before and after chugging showed a drop of about 10 percent in both average combustion-chamber pressure and in mean thrust under chugging conditions. Comparison of runs in which chugging occurred with runs at similar pressure settings and oxidant-fuel ratios in which chugging did not occur indicated increased propellant consumption and a decrease of specific impulse of more than 10 percent under chugging conditions.

Combustion time delay. - The experimental time delay between injection and combustion, θ in the theoretical analysis, was evaluated by averaging the measured time lags between flow maximums and pressure maximums, flow minimums and pressure minimums, and between both the increasing and diminishing mean flow and mean pressure values. The lag of the combustion-chamber pressure change behind the burning rate due to the necessity for changing the chamber volume was estimated from equation (A7) of appendix A and was subtracted from the measured time delay between flow and pressure response to find the combustion time delay. These combustion time delays for two rocket chambers of different characteristic lengths at a chamber pressure of approximately 270 pounds per square inch absolute are shown as related to the experimental chugging frequency in figure 5. The data for a 200-inch characteristic length rocket chamber correspond to several different sets of injector orifices. The combustion time delay decreased with increasing chugging frequency, and had values between 0.0027 and 0.0037 second for the 100-inch characteristic length rocket chamber and between 0.0052 and 0.0093 second for the 200-inch rocket chamber.

Shown on this same figure is the variation of the critical combustion time delay θ with chugging frequency based on the theoretical analysis. The dashed line shows the variation of chugging frequency with combustion time delay for engines of various characteristic lengths, but otherwise corresponding to the setup and operating conditions of the experimental engine. The experimentally observed combustion time delays are shorter than those predicted by the equations for corresponding chugging frequencies, although the curves follow the same trends. The combustion time delays observed for the 100-inch characteristic length rocket chamber were approximately one-half the values calculated from the analysis.

Effect of rocket combustion-chamber characteristic length. - The effect of rocket engine characteristic length L^* on the chugging frequency is shown in figure 6 for two rocket motors of different lengths but otherwise identical, that is, with the same injection head, chamber diameter, and exhaust nozzle, and operated at approximately the same chamber pressure. Plotted in this same figure are points calculated from the theoretical analysis. The experimental and analytical chugging frequencies in this case agree very closely. For example, the analytical chugging frequency for a characteristic length of 100 inches was 37 cycles per second; the experimentally obtained value was 38 cycles per second. The experimental chugging frequency decreased as the characteristic length was increased, as predicted by the analytical development.

Because there is no obvious reason for the actual combustion time delay to be affected by change in chamber characteristic length, it may be deduced that at the onset of chugging the mean combustion time delay seeks values which will permit chugging. Once initiated, the adjusted combustion time delay for the same injector configuration is different

for rockets of various characteristic lengths. The mean combustion time delay during chugging is also influenced by the particular injector configuration and to some extent by the amplitude of the chugging, as will be discussed.

Effect of throttling. - The experimental effect of varying the combustion-chamber pressure and thrust of a rocket engine by decreasing the pressurizing gas pressure is shown in figure 7. The experimental points indicate that the chugging frequency decreases with decrease in chamber pressure and thrust. This result is contradictory to the theoretical prediction. Results of calculations based on the analysis for a fixed configuration corresponding to the experimental rocket are shown on the plot as a dashed line. The fact that the ratio of the propellant-feed-system pressure drop to the absolute chamber pressure varies with the pressure for a fixed rocket configuration was taken into account in plotting the theoretical curve. The increase in ratio of pressure drop to chamber pressure ratio $\Delta p/p_c$ was considered proportional to the increase in chamber pressure.

The lack of correlation between the experimental and analytical chugging frequencies can be attributed to the following simplifying assumptions: (1) the combustion time delay is invariant throughout the chugging cycle, and (2) the chugging amplitudes are small. That the combustion time delay is unchanged under the changing flow and combustion pressure conditions existing during the chugging cycle is unlikely. In addition, the observed chugging amplitudes are high and probably limited by secondary or nonlinear damping effects or terms which do not appear in the analytical derivation, for example, the increase in propellant-feed-system pressure drop with increased amplitude of pulsing flow. Therefore, the experimental chugging rocket will not necessarily behave in accordance with the analytical equations but will be governed to some extent by those factors which were assumed negligible in the analysis in order to permit mathematical solution.

For a fixed rocket configuration, the injection and combustion of propellants are probably improved at higher chamber pressures and the combustion time delay would diminish. Thus increasing combustion-chamber pressure may increase the chugging frequency as observed for the experimental rocket.

Another factor which may affect chugging when the injection pressure drop and the chamber pressure are increased is the change in over-all combustion efficiency or specific impulse. A decrease in specific impulse decreases the chugging frequency for sustained chugging, in accordance with these observations. For the conditions of similar line length and fluid velocity, the analysis predicts that changing thrust would have no effect on chugging conditions.

Effect of injection velocity. - Chugging frequencies for a number of different injector orifice sets in a 200-inch characteristic length rocket chamber are plotted in figure 8 against the velocity of the acid jets. The data points show that as the velocity of the jets was increased the chugging frequency increased. Since the pressure drop across the injector orifices increases with increased velocity of the injection jets, the experimental chugging frequency can be said to increase with increased injector pressure drop. Again this relation is contrary to the theoretical prediction (shown as a dashed curve in fig. 8).

It is generally accepted that the combustion process may be affected by the injection process and that better atomizing and mixing can be accomplished by increased injection velocities. Thus the mean combustion time delay probably diminishes with increased injection velocity and the chugging frequency may increase. A change in combustion efficiency or specific impulse resulting from increased injector pressure may be a partial explanation of the observed results.

Effect of oxidant-fuel ratio. - Figure 9 is a plot of the chugging frequencies of several rocket-engine configurations, essentially several different injector orifice sizes, against over-all oxidant-fuel ratio. These data are for the 200-inch rocket operated at a chamber pressure of approximately 280 pounds per square inch absolute. The plotted data points indicate that the chugging frequency for each rocket configuration is substantially independent of oxidant-fuel ratio at constant rocket-chamber pressure. The analytical approach is based on a monopropellant model; consequently it affords no information of the effect of oxidant-fuel ratio.

The fact that most rocket engines involve two propellants and, correspondingly, two propellant systems introduces complications. The propellant systems are not likely to have similar dynamic characteristics; consequently a periodic variation during the chugging cycle of the oxidant-fuel ratio delivered to the combustion chamber probably occurs. If the rate of combustion of the propellants is a sensitive function of oxidant-fuel ratio, as well as of chamber pressure and temperature, which are functions of the oxidant-fuel ratio, then the combustion time delay will vary throughout the chugging cycle. Thus, it is evident that any stability criterion for the occurrence of chugging which is based strictly on pressure drop and feed system and chamber dimensions of the rocket engine without regard to the combustion process occurring in the engine may yield misleading indications. If the variation of the combustion rate is greater than the variation of the flow rate, the varying combustion rate can supply additional "gain" or amplification to the cycle to promote chugging under conditions for which, according to the analysis, chugging should be damped out. This factor may account for the intensity of some chugging runs.

Variation of chugging frequency with amplitude of chamber pressure fluctuations. - It was observed that when the chugging frequency for a particular rocket configuration varied during a run or from run to run there was a corresponding variation in the amplitude of the pressure fluctuations. The differences between maximum and minimum chamber pressures and the chugging frequencies for corresponding points are shown for a chugging run in figure 10. This chugging frequency decreased when the pressure differences increased.

The amplitude of pressure fluctuations for a number of runs of two rocket-engine configurations, different only in the sizes of the injector orifices, are plotted in figure 11 against the normal chugging frequencies. The chugging frequencies again decreased when the pressure fluctuations increased.

Large chamber-pressure fluctuations can occur during chugging operations. Pressure differences of 550 pounds per square inch at an average chamber pressure of 260 pounds per square inch have been observed during normal chugging.

Because this analysis is based on the assumption that the pressure fluctuations are negligible compared with their mean values, the effect of pressure amplitude on the chugging conditions is not predicted. However, if the chugging frequencies are in part dependent on the relative dynamic characteristics of the oxidant and fuel feed systems, a change of amplitude will affect the chugging frequency. More intense chugging would probably increase the mean combustion time delay which would result in reduced chugging frequencies, as indicated by the experimental data.

Evaluation of analysis. - The concept of time delay between injection and combustion of the propellants is confirmed by the measurements of the time delay between change of acid flow and change of combustion-chamber pressure. The analysis, based on this concept as a cause of chugging, gave calculated chugging frequencies of approximately correct magnitude and correctly predicted some trends of varying the rocket design and operating parameters. The agreement of magnitude of the predicted and observed chugging frequencies can be considered fortuitous in view of the simplifying assumptions made in deriving the end equations. Among the factors not previously discussed are: (1) the compressibility of the propellant and the flexibility of the propellant feed lines, both of which will permit oscillating conditions at higher frequencies, (2) the time for a pressure surge to travel from its point of origin to the nozzle, a factor of increasing importance at higher frequencies and for larger rocket chambers, (3) reflecting pressure waves in the chamber, (4) the inertia of the gas in the rocket chamber and nozzle, (5) nonisothermal conditions in the chamber during a chugging cycle, and (6) any accelerations of the rocket engine as a unit. Despite limitations imposed by these assumptions, the basic concepts of the analysis seem to be well founded and may lead to better understanding of the chugging phenomenon.

Although chugging in rocket engines has occurred primarily at low feed-system and injector pressure drops, the analysis indicates that stable operation at low pressure drops can be accomplished if the combustion time delay is sufficiently short. The actual combustion time delay probably has values of different magnitudes for different propellant combinations and injection methods; consequently, different chugging conditions and regimes will occur for different propellant combinations and for different injection methods.

SUMMARY OF RESULTS

Experimental runs with a 300-pound-thrust acid-heptane rocket engine having a pressurized-gas propellant pumping system showed:

1. Chugging frequencies of about 38 cycles per second were obtained for a 100-inch characteristic length rocket engine at a chamber pressure of 280 pounds per square inch. A frequency of 37 cycles per second was calculated from the analysis for this rocket engine.

2. Increasing combustion-chamber characteristic length decreased the chugging frequency, as predicted by the analysis.

3. Increasing chamber operating pressure (fixed configuration) or increasing propellant-line pressure drop increased the chugging frequencies. These trends were incorrectly predicted by the analysis; the disagreement is attributed to the simplifying assumption of constant combustion time delay.

4. No apparent effect of oxidant-fuel ratio on the chugging frequency for acid-heptane ratios from 3.0 to 7.0 occurred. No effect is predicted by the analysis, which assumes a monopropellant system.

5. The chugging frequencies decreased with increased amplitude of chugging. The analysis makes no prediction of the effect of pressure amplitude on chugging frequency because the pressure fluctuations were assumed negligible.

Lewis Flight Propulsion Laboratory
National Advisory Committee for Aeronautics
Cleveland, Ohio, July 1, 1951

APPENDIX A

ANALYSIS OF LOW-FREQUENCY VIBRATIONS

The fundamental concepts on which the analysis of low-frequency chugging vibrations is based are discussed in the main body of this report. The analysis is based on the concept of a hydraulic coupling between the flow of a monopropellant from its storage tank to the rocket chamber and the rocket combustion-chamber pressure. Surges of the propellant flow and the chamber pressure are promoted by a time interval or lag between each change of propellant flow and the corresponding change of pressure. This time interval comprises (1) the delayed response of the flow to any change of chamber pressure due to the inertia of the fluid, called the inertia time lag, (2) a time delay between propellant injection and actual combustion, called the combustion time delay, and (3) a time difference between a change in combustion rate and the corresponding change in chamber pressure, called the charging time lag.

Although the inertia time lag and the charging time lag can be expressed mathematically as functions of the feed line and chamber geometry and the chugging frequency, this analysis assumed that the combustion time delay is constant because of lack of information on the dynamics or kinetics of factors which influence it. Probably the combustion time delay is influenced by factors such as varying degrees of atomization, mixing, the vaporizing due to variation in the injector pressure drop with the propellant flow surges, and the varying combustion-chamber pressure. Some interpretation of the parameters which determine and influence chugging is possible despite the limitations imposed by the assumptions.

ASSUMPTIONS

The cycle can be treated mathematically for a monopropellant if the following assumptions are made:

(1) The liquid propellant burns instantly into gaseous products at a definite time after being injected into the rocket combustion chamber, that is, the combustion time delay is constant.

(2) The propellant has negligible volume while in the unburned phase in the combustion chamber.

(3) The amplitudes of the cyclical variations in combustion-chamber pressure and propellant flow are small compared with their mean values and the variations in flow can be expressed by sinusoidal equations.

(4) The propellant is incompressible and the propellant feed system is inflexible.

DERIVATION OF EQUATIONS

The first assumption implies that the rate of combustion of the propellant at time t is equal to the rate of propellant injection into the rocket combustion chamber at some previous time $(t - \theta)$.

$$W_b \text{ at } (t) = W_i \text{ at } (t - \theta) \tag{A1}$$

The gaseous combustion products in the rocket combustion chamber are proportional to the combustion-chamber pressure. The volume occupied by the unburned propellants is considered negligible (assumption (2)) and the combustion temperature is considered constant. The small variations in the chamber pressure (assumption (3)) are considered not to affect the combustion temperature

$$m_g = \frac{V_c \, p_c}{R \, T_c} = K_1 \, p_c \tag{A2}$$

Differentiation gives

$$\frac{dm_g}{dt} = K_1 \frac{dp_c}{dt} \tag{A3}$$

If the inflow and outflow of gas in the rocket combustion chamber are considered

$$\frac{dm_g}{dt} = W_b - W_g \tag{A4}$$

If (A3) and (A4) are combined,

$$W_b - W_g = K_1 \frac{dp_c}{dt} \tag{A5}$$

The flow from the rocket exhaust nozzle W_g depends on the combustion gas density which, with constant temperature combustion gas, is proportional to the chamber pressure

$$W_g = K_2 \, p_c \tag{A6}$$

If (A5) and (A6) are combined,

$$W_b = K_2 p_c + K_1 \frac{dp_c}{dt} \tag{A7}$$

The chamber pressure can be expressed in terms of the propellant tank pressure and fuel-system pressure drops. The instantaneous pressure drop from the rocket propellant tank to the combustion chamber comprises three terms: (1) the drop across the propellant injection orifices, (2) the friction in the propellant feed line, and (3) the inertia of the propellant in the feed system.

The injection-orifice pressure drop has the form of an orifice equation

$$W_i = K_3 (p_i - p_c)^{1/2} \tag{A8}$$

The general form of the friction pressure drop is

$$\Delta p_f = \frac{f v^2 l \rho}{2g D} \tag{A9}$$

This equation applies only in the turbulent region of fluid flow. At high Reynolds numbers such as occur in the propellant feed line the friction factor f is a relatively insensitive function of fluid velocity and may be considered constant for small variations in propellant flow (assumption (3)). Equation (A9) then becomes

$$\Delta p_f = F v^2 \tag{A10}$$

The difference between the pressure force from propellant tank to injector orifice and the force required to overcome friction in the line is due to inertia forces

$$(p_t - p_i) - F v^2 = \frac{\rho l}{g} \frac{dv}{dt} \tag{A11}$$

The equation for the pressure drop from propellant tank to combustion chamber is then

$$p_t - p_c = \frac{W_i^2}{K_3^2} + F v^2 + \frac{\rho l}{g} \frac{dv}{dt} \tag{A12}$$

But since

$$v = \frac{W_i}{\rho a} \tag{A13}$$

and

$$\frac{dv}{dt} = \frac{1}{\rho a} \frac{dW_i}{dt} \tag{A14}$$

the chamber pressure is

$$p_c = p_t - \frac{W_i^2}{K_3^2} - F\left(\frac{W_i}{\rho a}\right)^2 - \frac{l}{ga} \frac{dW_i}{dt} \tag{A15}$$

If the instantaneous flow rate W_i is assumed to comprise a steady flow W_o and an unsteady term represented as a function of time

$$W_i = W_o + f(t) \tag{A16}$$

$$W_i^2 = W_o^2 + 2W_o\, f(t) + f^2(t) \tag{A17}$$

Assumption (3) permits the term $f^2(t)$ to be neglected.

Equation (A15) then becomes

$$p_c = p_t - \frac{W_o^2}{K_3^2} - \frac{2W_o\, f(t)}{K_3^2} - \frac{FW_o^2}{(\rho a)^2} - \frac{2F\, W_o\, f(t)}{(\rho a)^2} - \frac{l}{ga} \frac{df(t)}{dt} \tag{A18}$$

and

$$\frac{dp_c}{dt} = - \frac{2W_o\, df(t)}{K_3^2\, dt} - \frac{2F\, W_o}{(\rho a)^2} \frac{df(t)}{dt} - \frac{l}{ga} \frac{d^2 f(t)}{dt^2} \tag{A19}$$

If

$$W_i = W_o + f(t)$$

then from equation (A1)

$$W_b = W_o + f(t - \theta) \tag{A20}$$

Equation (A7) can be combined with equations (A18) and (A19)

$$W_o + f(t - \theta) = K_2 \left[p_t - \frac{W_o^2}{K_3^2} - \frac{2W_o\, f(t)}{K_3^2} - \frac{F\, W_o^2}{(\rho a)^2} - \frac{2F\, W_o\, f(t)}{(\rho a)^2} - \frac{l}{ga}\frac{df(t)}{dt} \right] +$$

$$K_1 \left[- \frac{2W_o}{K_3^2}\frac{df(t)}{dt} - \frac{2F\, W_o}{(\rho a)^2}\frac{df(t)}{dt} - \frac{l}{ga}\frac{d^2f(t)}{dt^2} \right] \tag{A21}$$

which can be rewritten

$$K_1 \frac{l}{ga}\frac{d^2f(t)}{dt^2} + \left(K_1 \frac{2W_o}{K_3^2} + K_1 \frac{2F\, W_o}{(\rho a)^2} + K_2 \frac{l}{ga} \right) \frac{df(t)}{dt} +$$

$$\left(K_2 \frac{2W_o}{K_3^2} + K_2 \frac{2F\, W_o}{(\rho a)^2} \right) f(t) + f(t - \theta)$$

$$= K_2\, p_t - \frac{K_2}{K_3^2} W_o^2 - \frac{K_2\, F\, W_o^2}{(\rho a)^2} - W_o \tag{A22}$$

The right-hand side of this equation can be shown to equal zero by using mean values in equation (A15)

$$\overline{p_t} - \overline{p_c} = \frac{W_o^2}{K_3^2} + \frac{F\, W_o^2}{(\rho a)^2} \tag{A23}$$

Multiplying all terms by K_2 and combining with equation (A6) yield

$$K_2 \overline{p_t} - \frac{K_2 W_o^2}{K_3^2} - K_2 \frac{F W_o^2}{(\rho a)^2} - W_o = 0 \tag{A24}$$

The remainder of equation (A22) can be written

$$A \frac{d^2 f(t)}{dt} + B \frac{df(t)}{dt} + Cf(t) + f(t - \theta) = 0 \tag{A25}$$

where

$$A = \frac{K_1 l}{ga} \tag{A26}$$

$$B = \left(\frac{K_1 2W_o}{K_3^2} + \frac{K_1 2F W_o}{(\rho a)^2} + \frac{K_2 l}{ga} \right) \tag{A27}$$

$$C = \left(\frac{K_2 2W_o}{K_3^2} + \frac{K_2 2F W_o}{(\rho a)^2} \right) \tag{A28}$$

Equation (A25) governs chugging vibrations in the rocket combustion chamber, provided the assumptions are valid, and can be solved if $f(t)$ is assumed to follow a sinusoidal curve such that

$$f(t) = Se^{nt} \sin \omega t \tag{A29}$$

If n is positive the vibrations will have increasing amplitude; if n is negative the vibrations will be damped. S is an amplitude factor.

The term e^{nt} can be expanded into a series

$$e^{nt} = 1 + nt + \frac{(nt)^2}{2!} + \frac{(nt)^3}{3!} + \ldots \tag{A30}$$

Because interest for the case of sustained chugging vibrations lies in values of n near zero all terms beyond nt in equation (A30) can be dropped.

Then

$$f(t) = S \sin \omega t + S\, nt \sin \omega t \tag{A31}$$

$$\frac{df(t)}{dt} = S\omega \cos \omega t + S\omega\, nt \cos \omega t + S\, n \sin \omega t \tag{A32}$$

$$\frac{d^2f(t)}{dt^2} = - S\omega^2 \sin \omega t - S\omega^2\, nt \sin \omega t + S\omega n \cos \omega t + S\omega n \cos \omega t \tag{A33}$$

$$f(t - \theta) = (1 + nt - n\theta) \left[S \sin (\omega t - \omega\theta) \right] \tag{A34}$$

$$f(t - \theta) = (1 + nt - n\theta) \left[S \sin \omega t \cos \omega\theta - S \cos \omega t \sin \omega\theta \right] \tag{A35}$$

Substituting these values in equation (A25) and combining terms with like coefficients of t give

$$\left[-A\omega^2 + Bn + C + (1 - n\theta) \cos \omega\theta \right] \sin \omega t +$$

$$\left[2A\omega n + B\omega - (1 - n\theta) \sin \omega\theta \right] \cos \omega t +$$

$$\left[-A\omega^2 + C + \cos \omega\theta \right] nt \sin \omega t +$$

$$\left[B\omega - \sin \omega\theta \right] nt \cos \omega t = 0 \tag{A36}$$

Because the equation is valid for all values of t the coefficient of each term must be independently equal to zero.

Evaluation of Constants

The constants A, B, and C must be evaluated in terms of commonly used rocket parameters.

From equation (A26)

$$A = \frac{K_1 \, l}{ga}$$

$$K_1 = \frac{m_g}{p_c} = \frac{V_c \, \rho_c}{p_c} \tag{A37}$$

Because the volume of the combustion chamber is equal to the characteristic length times the throat area of the rocket nozzle,

$$K_1 = \frac{L^* \, a_t \, \rho_c}{p_c} \tag{A38}$$

From isentropic nozzle flow theory,

$$a_t = \frac{W_o}{\overline{\rho_t} \, c_t} \tag{A39}$$

where

$$c_t = \sqrt{\frac{2\gamma}{\gamma + 1} gR \frac{T_c}{M}} \tag{A40}$$

and

$$\overline{\rho_t} = \overline{\rho_c} \left(\frac{2}{\gamma + 1} \right)^{\frac{1}{\gamma - 1}} \tag{A41}$$

Thus

$$a_t = \frac{W_o}{\overline{\rho_c} \sqrt{\left(\frac{2}{\gamma + 1} \right)^{\frac{\gamma+1}{\gamma-1}} \gamma g R \frac{T_c}{M}}} \tag{A42}$$

Therefore

$$K_1 = \frac{L^* W_o}{\overline{p_c}\sqrt{\left(\frac{2}{\gamma+1}\right)^{\frac{\gamma+1}{\gamma-1}} \gamma g R \frac{T_c}{M}}} \tag{A43}$$

and

$$A = \frac{L^* W_o}{\overline{p_c}\sqrt{\left(\frac{2}{\gamma+1}\right)^{\frac{\gamma+1}{\gamma-1}} \gamma g R \frac{T_c}{M}}} \frac{l}{ga} \tag{A44}$$

Combining equation (A27) with equations (A43), (A8), and (A6) gives

$$B = \frac{2L^*}{\overline{p_c}\sqrt{\left(\frac{2}{\gamma+1}\right)^{\frac{\gamma+1}{\gamma-1}} \gamma g R \frac{T_c}{M}}} \left[(\overline{p_i} - \overline{p_c}) + \frac{F}{(\rho a)^2} W_o^2\right] + \frac{W_o}{p_c} \frac{l}{ga} \tag{A45}$$

Combining equation (A28) with equations (A8) and (A6) results in

$$C = \frac{2}{\overline{p_c}} \left[(\overline{p_i} - \overline{p_c}) + \frac{F}{(\rho a)^2} W_o^2\right] \tag{A46}$$

The expressions for the constants B and C involve an expression

$$\left[(\overline{p_i} - \overline{p_c}) + \frac{F W_o^2}{(\rho a)^2}\right]$$

This term comprises the pressure drops from the tank to the combustion chamber. Evidently, if incompressible fluid and inflexible propellant feed lines are assumed, the pressure drop in the feed lines can be added to the injector pressure drop.

$$(\overline{p_i} - \overline{p_c}) + F\,\overline{v}^2 = \overline{\Delta p} \tag{A47}$$

Thus

$$B = \frac{2L^*}{\overline{p_c}\sqrt{\left(\frac{2}{\gamma+1}\right)^{\frac{\gamma+1}{\gamma-1}}\gamma g R\,\frac{T_c}{M}}}\,\overline{\Delta p} + \frac{W_o\,l}{\overline{\overline{p_c}}\,ga} \tag{A48}$$

and

$$C = \frac{2}{\overline{\overline{p_c}}}\,\overline{\Delta p} \tag{A49}$$

SUMMARY AND DISCUSSION OF EQUATIONS

The analysis yields an expression of the following form for chugging in a rocket engine:

$$A\,\frac{d^2f(t)}{dt^2} + B\,\frac{df(t)}{dt} + Cf(t) + f(t - \theta) = 0 \tag{A25}$$

This expression for chugging operation in which there is no change in chugging amplitude can be solved by using two simultaneous equations

$$-A\omega^2 + C + \cos \omega\theta = 0$$

$$B\omega - \sin \omega\theta = 0$$

where

θ combustion time delay, sec

ω chugging frequency, radians/sec

$$A = \frac{L^* W_o}{\overline{p_c}\sqrt{\left(\frac{2}{\gamma+1}\right)^{\frac{\gamma+1}{\gamma-1}} \gamma g R \frac{T_c}{M}}} \frac{l}{ga} \tag{A44}$$

$$B = \frac{2L^* \overline{\Delta p}}{\overline{p_c}\sqrt{\left(\frac{2}{\gamma+1}\right)^{\frac{\gamma+1}{\gamma-1}} \gamma g R \frac{T_c}{M}}} + \frac{W_o}{\overline{p_c}} \frac{l}{ga} \tag{A48}$$

$$C = \frac{2\overline{\Delta p}}{\overline{p_c}} \tag{A49}$$

Solution of the two simultaneous equations yields values of the combustion time delay θ and the cycling frequency ω which delineate the chugging from the nonchugging conditions of rocket operation and correspond to operation at a condition where no change of chugging amplitude occurs. The calculated value of the combustion time delay represents the minimum combustion time delay at which chugging can be sustained. Chugging at longer combustion time delays is possible, but the chugging amplitude will increase with each cycle or will be limited by secondary or nonlinear damping terms which do not appear in the equations and the equations of the analysis would no longer apply.

The equations describe a feedback system in which no amplification or gain of the feedback loop is accomplished except through the hydrodynamics and phase relations of the system.

Application of Analysis

A typical example has been set up and the equations applied to determine the effect on critical combustion time delay and stable chugging frequency of changes in the following variables: ratio of propellant feed-line pressure drop to the rocket-chamber pressure, characteristic length, combustion-chamber pressure, propellant feed-line length and area, and thrust.

Values of rocket operating and design parameters are listed in the following discussion. The results are plotted in figures 12 to 21 in terms of the variation of the critical combustion time delay and calculated chugging frequency as functions of the parameter varied.

The following conditions were chosen as standard, some of which were taken from the experimental performance of white fuming nitric acid and heptane:

Ratio of specific heats, γ	1.22
Ratio of combustion temperature to molecular weight of propellant gases, T_c/M, $^\circ R/mol$	214
Specific impulse, I, lb-sec/lb	187.5
Propellant density, ρ, lb/cu ft	93
Universal gas constant, R, ft-lb/$^\circ$R/mol	1544

These parameters were fixed and the following parameters were varied to determine their effect on the predicted vibration range. The values listed are those used when that particular parameter was not being varied. The following parameters were those corresponding to the 300-pound thrust acid-heptane experimental rocket engine:

Rocket engine thrust, T, lb	300
Combustion-chamber pressure, p_c, lb/sq in. abs.	300
Characteristic length, L^*, in.	100
Length of propellant feed line, l, ft	4
Cross-sectional area of propellant feed line, a, sq in.	0.2485
Pressure drop due to friction, Δp_f, lb/sq in.	20

Effect of change of ratio of total propellant feed-system pressure drop to rocket combustion-chamber absolute pressure. - The effect of change of the ratio of total propellant feed-system pressure drop to the rocket combustion-chamber absolute pressure $\Delta p/p_c$ is shown in figures 12 and 13. The figures show that the critical combustion time delay will increase and the stable chugging frequency will decrease as the ratio $\Delta p/p_c$ is increased. Figure 12 indicates for each value of $\Delta p/p_c$ a minimum combustion time delay for chugging to occur. Figure 12 indicates that the combustion time delay becomes infinitely large and the stable chugging frequency approaches a value of zero as the ratio of $\Delta p/p_c$ approaches a value of 0.5. A practical limitation is realized before this condition can pertain, however. The maximum values which the combustion time delay θ can have are uncertain but they must be less than the "stay time" of the propellant in the rocket chamber; that is, they must be less than 0.01 second for most rocket configurations. The analytical derivation shows that if the combustion time delay is sufficiently small (0.003 sec for the rocket configuration for which the analytical results are plotted) the rocket cannot chug at any value of $\Delta p/p_c$.

Effect of varying characteristic length. - The effect of varying rocket chamber characteristic length L^* is shown in figures 14 and 15. The family of curves plotted are for an acid-heptane rocket with total propellant feed-system pressure drop equal to 0.3, 0.2, and 0.1 of the chamber pressure.

The curves delineate the chugging and nonchugging regions. Figure 14 indicates the combustion time delay for stable or sustained chugging with no amplitude change. Figure 15 shows the corresponding chugging frequency. An increase in the characteristic length causes an increase in the critical combustion time delay factor and a decrease in the corresponding chugging frequency for stable chugging operation. This combustion time delay increase is in addition to the increase in charging time of the chamber.

The chugging frequency for stable or sustained chugging for a rocket chamber characteristic length of 25 inches at $\Delta p/p_c = 0.2$ with other parameters as listed in previous discussion was 52 cycles per second; for a characteristic length of 100 inches the frequency was 37 cycles per second; for 200 inches the frequency was 27 cycles per second.

Effect of varying rocket combustion-chamber pressure. - The effect of varying the rocket combustion-chamber pressure is considered for (1) a rocket configuration in which the thrust is kept constant, and (2) throttling a fixed rocket configuration by changing the pumping pressure in which case the engine thrust as well as the pressure is varied.

The effect of varying the rocket combustion-chamber pressure on the chugging frequency of a rocket engine configuration in which the thrust is kept constant by adjusting the nozzle throat area (and the combustion chamber volume so as to maintain constant L^*) is shown in figures 16 and 17. The constants used in the equations neglect the change in specific impulse with increased rocket chamber pressure. For this case the analysis predicts that as the combustion-chamber pressure is increased the critical combustion time delay for sustained chugging will decrease; that is, the chugging frequency will increase. Figure 16 shows that the critical combustion time delay decreases as the rocket chamber pressure increases. If the combustion time delay remains constant as the operating pressure is increased then chugging is more likely to occur at higher chamber pressures; that is, if the rocket configuration used for this illustration has a combustion time delay of 0.004 second and a $\Delta p/p_c$ ratio of 0.2, then chugging may occur if the chamber pressure is 400 pounds per square inch or greater. However, the actual combustion time delay probably decreases as the chamber pressure increases. The computed stable chugging frequency for the assumed rocket configuration for $\Delta p/p_c = 0.2$ was about 16 cycles per second at 100 pounds per square inch absolute; at 1000 pounds per square inch it was 66 cycles per second.

For a rocket engine of fixed configuration which is throttled by changing the tank pressures, figures 16 and 17 do not apply. For a fixed configuration, varying the chamber pressure changes the thrust and the

velocity of the propellant flow in the feed line as well as the ratio of $\Delta p/p_c$. For a constant ratio of $\Delta p/p_c$ the combustion time delay for sustained chugging can be shown to be nearly unaffected by increased combustion-chamber pressure and thrust; consequently the resultant effect in a fixed rocket configuration is due primarily to change in the ratio of the total feed-system pressure drop to the absolute chamber pressure $\Delta p/p_c$. If the total feed-system pressure drop is assumed proportional to the square of the propellant flow rate and the propellant flow rate is assumed directly proportional to the chamber pressure, $\Delta p/p_c$ will vary directly as the chamber pressure.

Effect of varying propellant feed-line length and area. - The effects of varying the propellant feed-line length and area are shown in figures 18 and 19, respectively. In these figures the friction pressure drop through the 4-foot feed line was taken as 20 pounds per square inch and the $\Delta p/p_c$ ratio was assumed to be 0.2 for the standard configuration. The pressure drop was varied in proportion to the propellant feed-line length and in inverse proportion to the fifth power of the feed-line diameter $\left(\Delta p_f \propto \frac{1}{a^{2.5}}\right)$. The figures, therefore, show a double effect, that is, the effect of the parameter which was varied and the effect of changing friction pressure drop. Increasing the propellant-line length beyond about 23 feet increased the ratio of $\Delta p/p_c$ (because of increase of Δp_f) to a value greater than 0.5. The equations predict that chugging is impossible beyond this value of $\Delta p/p_c$. Restricting the line area to values less than about 0.13 square inch for the rocket configuration assumed had a similar effect (figs. 20 and 21). Shortening the propellant-line length or increasing the line area will increase the stable chugging frequency, as might be anticipated, because of the decrease in feed-line inertia.

Effect of varying engine thrust. - When thrust of a rocket engine is increased the propellant feed line geometry is generally changed to accommodate the increased propellant flow. Whether or not these changes affect chugging depends on the propellant line length, propellant velocity, and total pressure drop through the feed system. If these factors remain constant then an increase in thrust rating (engine size or scale) will not affect the chugging conditions. The restriction that these factors remain constant, however, is seldom realized in changing the scale of an engine. For example, in the case where the propellant-line area is increased to maintain constant propellant velocity, the friction pressure drop per unit length of line decreases as the inverse square root of the area. Inasmuch as the friction pressure drop is generally small compared with the injector pressure drop, the influence of its change on the total feed-system pressure drop and consequently on chugging would be of secondary importance in most cases. The effect of engine scale on the combustion processes and the influence of combustion effects on chugging are not considered.

The effect of varying thrust by throttling an engine has been discussed with the effect of changing combustion-chamber pressure.

SUMMARY OF RESULTS OF ANALYSIS

A simplified analysis of chugging in a rocket engine which uses a pressurized-gas propellant pumping system was based on the concept of a constant time delay between injection and combustion of the propellant. The analysis indicated:

(1) Increasing the propellant-line total pressure drop increases the critical combustion time delay and decreases the stable chugging frequency.

(2) A combustion time delay exists below which chugging is impossible at any value of feed-system pressure drop.

(3) Increase of chamber characteristic length increases the critical combustion time delay required for sustained chugging and decreases the stable (no change of amplitude) chugging frequency.

(4) An increase in chamber pressure for rocket engines in which the propellant velocity in the feed line is constant causes a decrease in the critical combustion time delay and an increase in stable chugging frequencies; throttling a fixed configuration by decreasing the tank pressures decreases the critical combustion time delay and increases the chugging frequency.

(5) Increasing the propellant-line length or decreasing the propellant-line area increases the critical combustion time delay and decreases the stable chugging frequency.

(6) Increasing the thrust of a rocket engine does not affect the critical combustion time delay or the stable chugging frequency provided the propellant-line fluid velocity and line length remain constant.

(7) Chugging frequencies of 37 cycles per second were calculated for a 300-pound thrust acid-heptane rocket of 100-inch characteristic length at a chamber pressure of 300 pounds per square inch absolute.

APPENDIX B

SYMBOLS

The following symbols are used in this report:

A,B,C	constants
a	cross-sectional area of propellant feed line, sq ft
a_t	rocket nozzle throat area, sq ft
c_t	combustion gas velocity at rocket nozzle throat, ft/sec
D	diameter of propellant feed line, ft
F	friction constant, $\frac{f\,l\,\rho}{2g\,D}$
f	fluid-friction factor
f(t)	function of time
g	gravitational acceleration, ft/sec^2
I	specific impulse, lb-sec/lb
K_1, K_2, K_3	constants
L*	characteristic length, combustion volume divided by throat area, ft
l	length of propellant feed line, ft
M	molecular weight of propellant gases, lb/mol
m_g	mass of burned propellant in combustion chamber, lb
n	exponential damping factor
p_c	combustion-chamber pressure, lb/sq ft
p_i	pressure at upstream face of propellant injector, lb/sq ft
p_t	propellant supply-tank pressure, lb/sq ft

Δp	$p_t - p_c$, lb/sq ft
Δp_f	pressure drop due to friction, lb/sq ft
R	universal gas constant, ft-lb/$^{\circ}$R/mol
S	amplitude factor
T	rocket engine thrust, lb
T_c	combustion temperature, $^{\circ}$R
t	time, sec
V_c	volume of combustion chamber, cu ft
v	velocity of fluid in propellant feed line, ft/sec
W_b	propellant burning rate, lb/sec
W_g	flow rate of combustion gas through exhaust nozzle, lb/sec
W_i	propellant flow rate at injector, lb/sec
W_o	mean propellant flow rate, lb/sec
γ	ratio of specific heats
θ	time delay between injection and combustion, sec
ρ	propellant density, lb/cu ft
ρ_c	combustion gas density, lb/cu ft
ρ_t	combustion gas density at rocket nozzle throat, lb/cu ft
ω	chugging frequency, radians/sec

Bar indicates mean value.

REFERENCES

1. Bellman, Donald R., and Humphrey, Jack C.: Photographic Study of Combustion in a Rocket Engine. I - Variation in Combustion of Liquid Oxygen and Gasoline with Seven Methods of Propellant Injection. NACA RM E8F01, 1948.

2. Gunder, D. F., and Friant, D. R.: Stability of Flow in a Rocket Motor. Jour. Appl. Mech., vol. 17, no. 3, Sept. 1950, pp. 327-333.

3. Yachter, M., and Waldinger, H. V.: Dynamic Analysis of a Rocket Motor. Rep. SPD-241, Spec. Proj. Dept., M. W. Kellogg Co., Oct. 1, 1949. (U. S. Navy, Bur. Aero., Contract NOa(s)-9498.)

4. Jaffe, Leonard, Coss, Bert A., and Daykin, Donald R.: An Electromagnetic Flowmeter for Rocket Research. NACA RM E50L12, 1950.

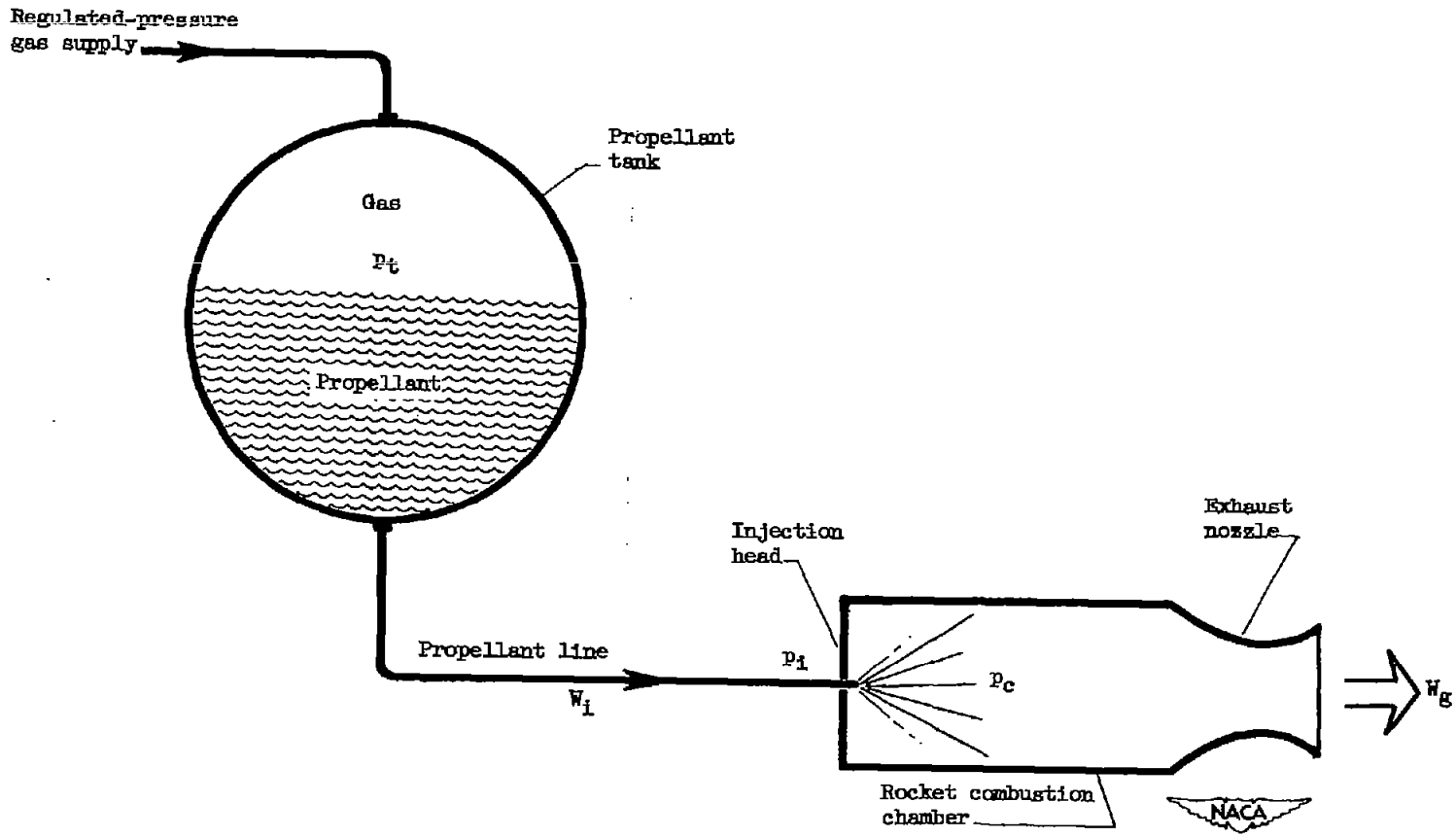

Figure 1. - Diagram of monopropellant rocket engine with pressurized-gas propellant pumping system.

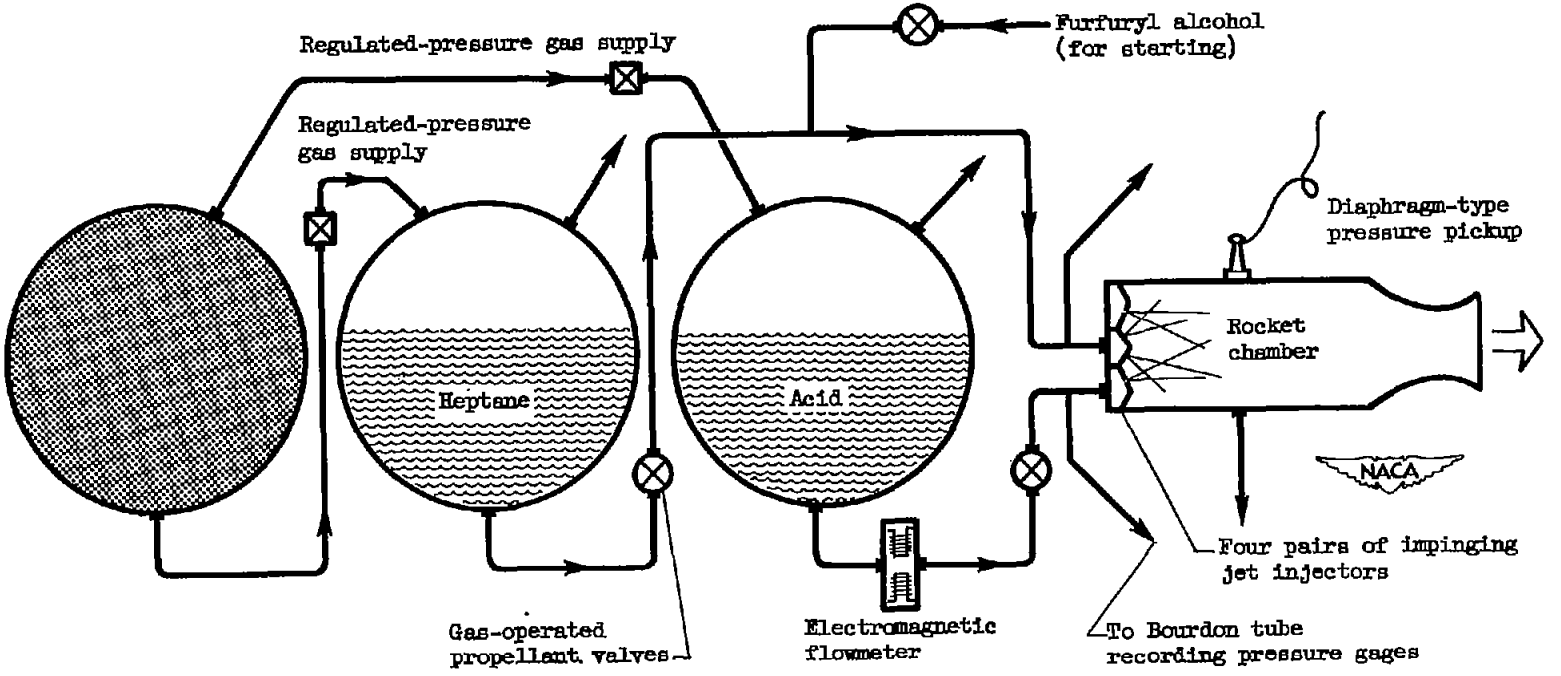

Figure 2. - Diagram of experimental 300-pound thrust acid-heptane rocket.

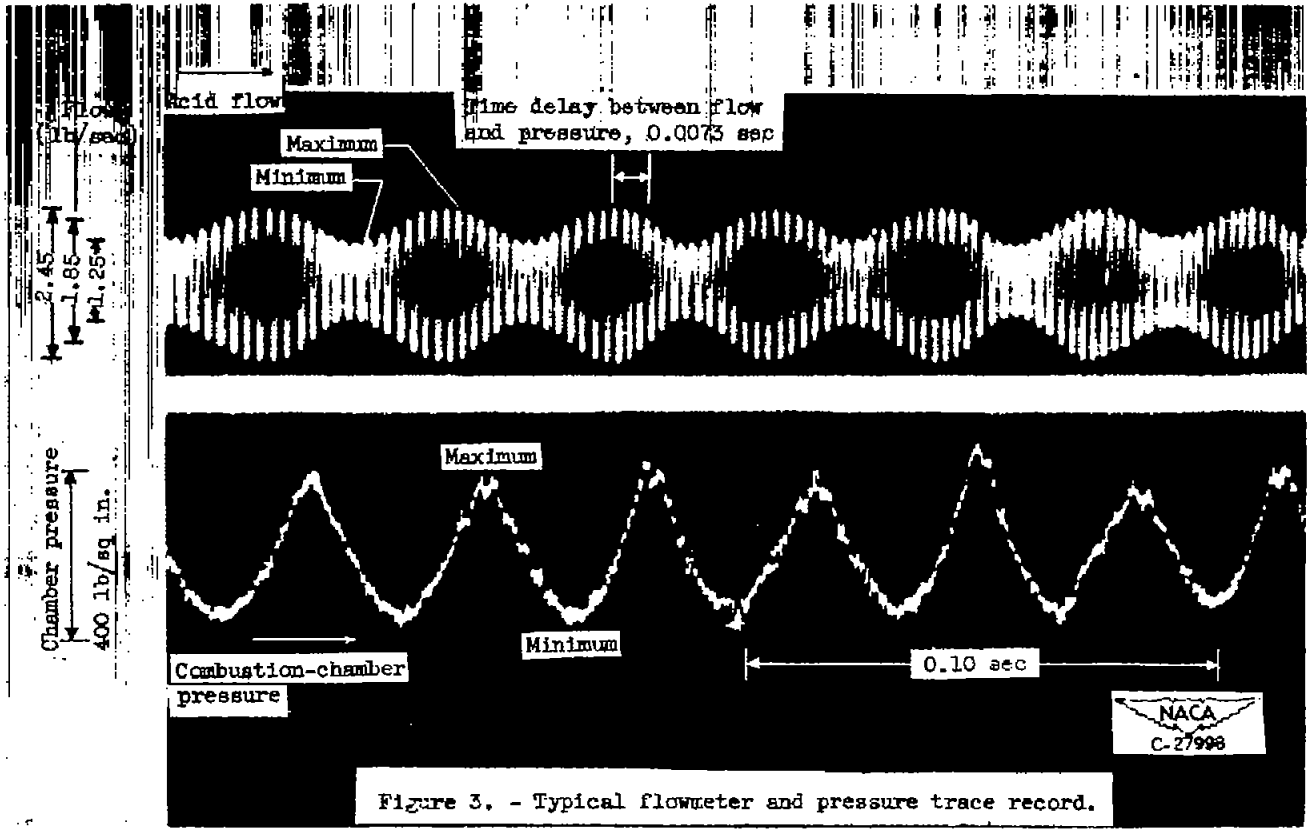

Figure 3. - Typical flowmeter and pressure trace record.

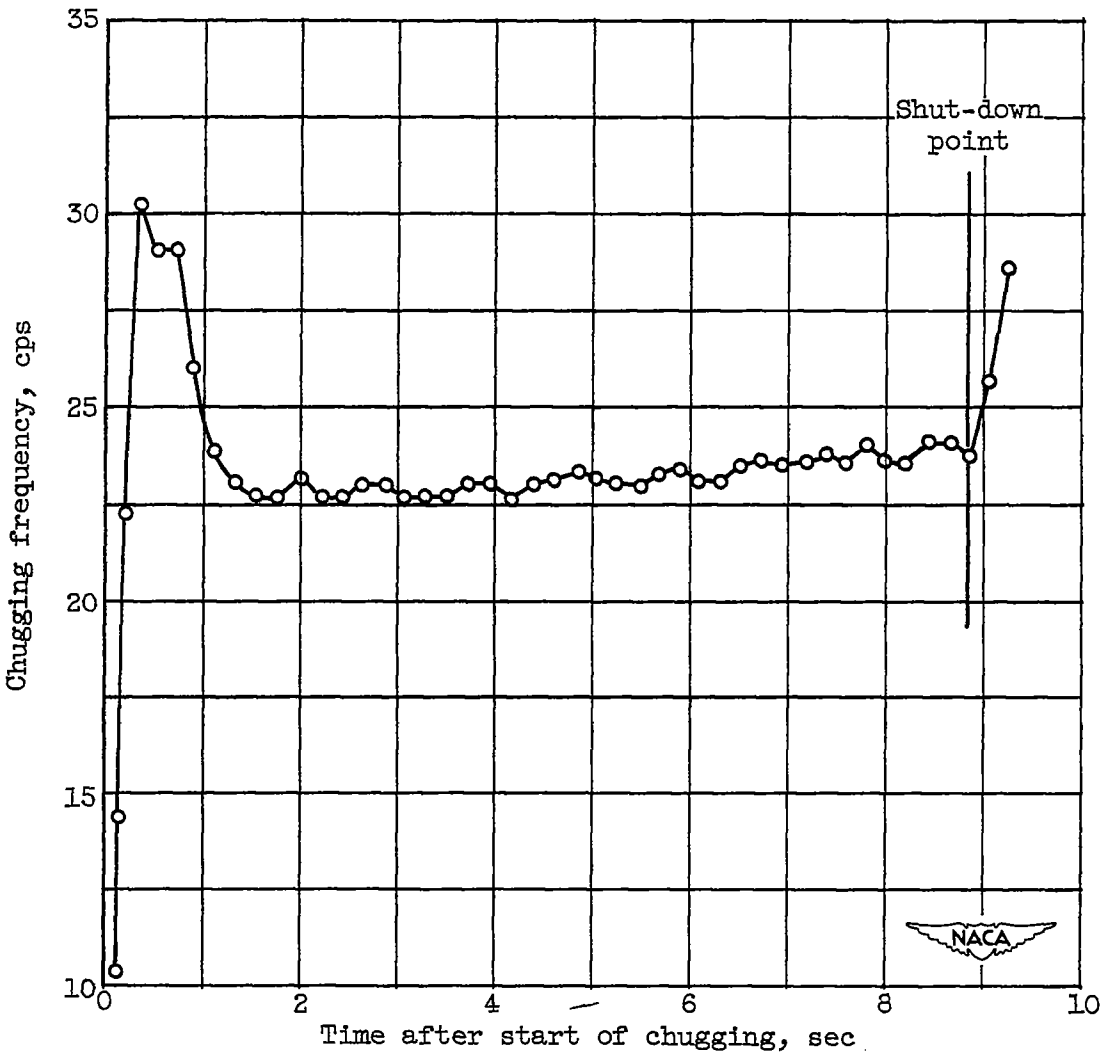

Figure 4. - Experimental variation of chugging frequency with time after start of chugging. Rocket chamber characteristic length, 200 inches; average chamber pressure, 250 pounds per square inch absolute.

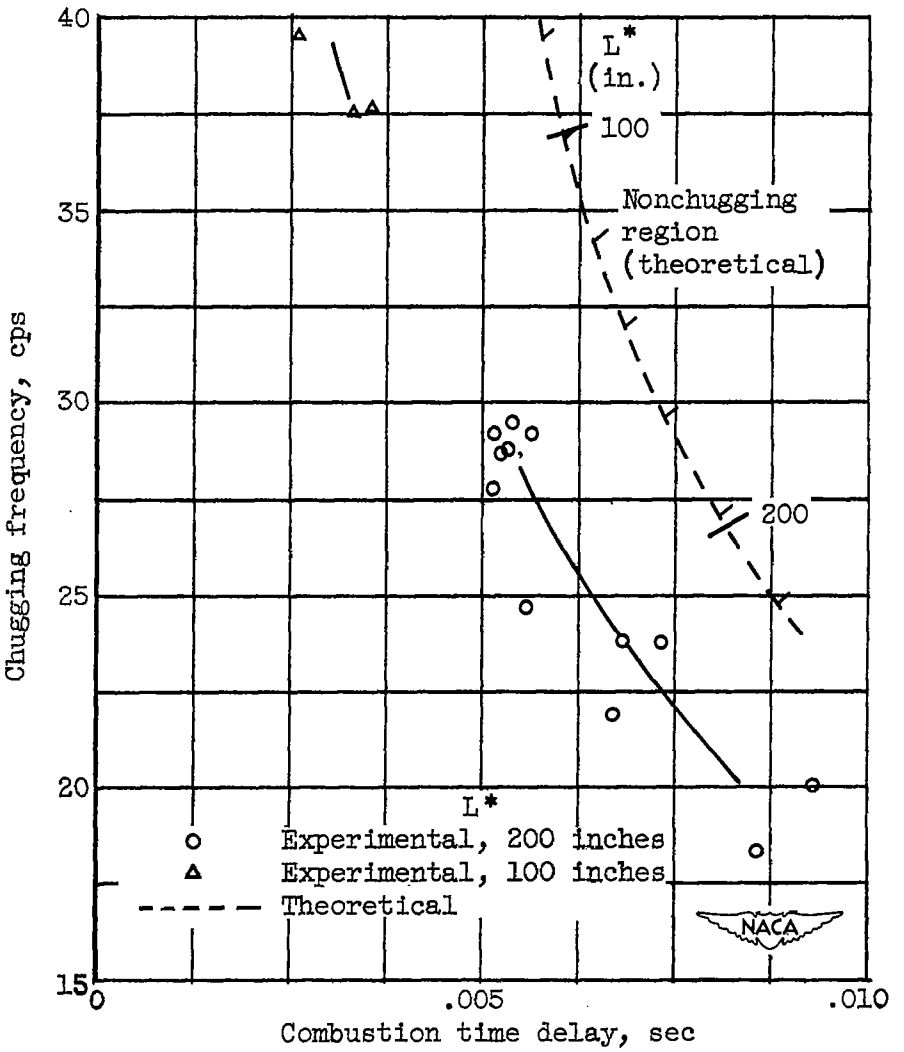

Figure 5. - Experimental variation of chugging frequency with time delay between propellant injection and combustion for two rocket chambers. Average chamber pressure, 270 pounds per square inch absolute.

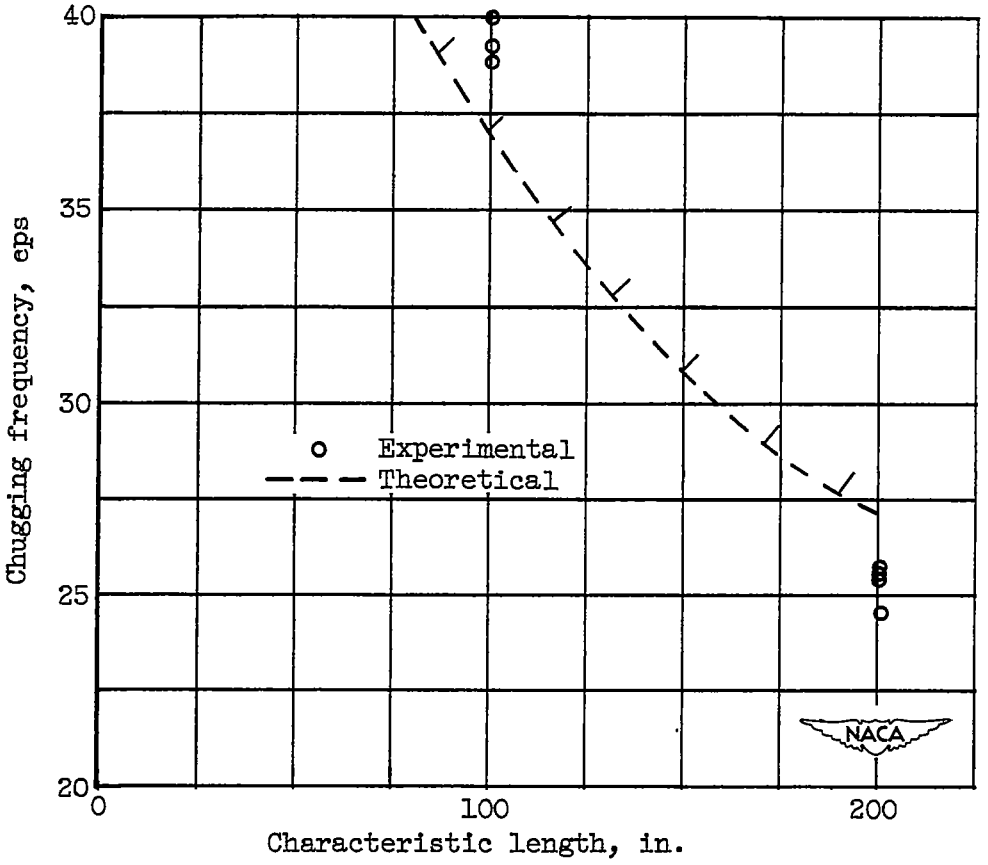

Figure 6. - Experimental variation of chugging frequency with rocket combustion-chamber characteristic length. Average chamber pressure, 270 pounds per square inch absolute.

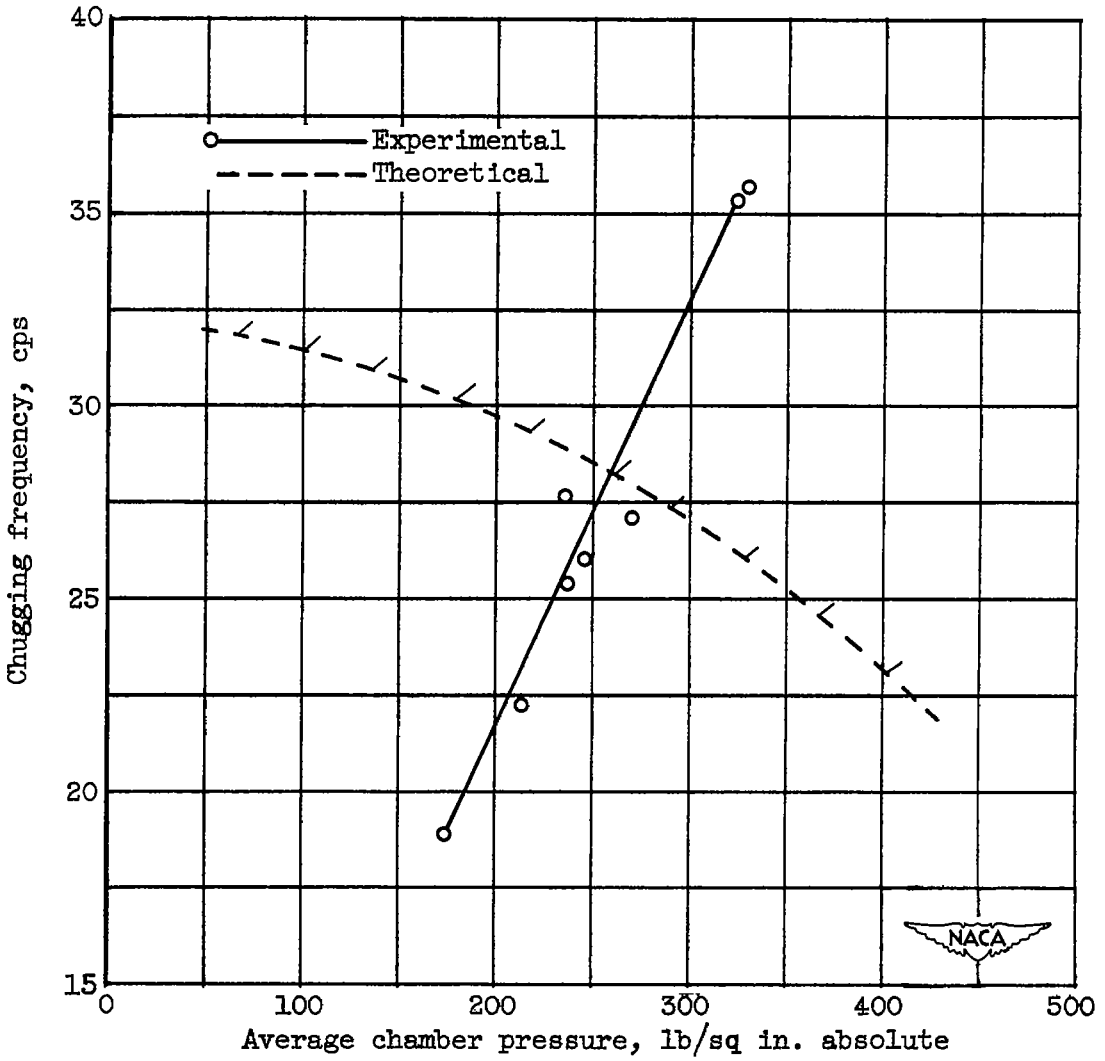

Figure 7. - Experimental variation of chugging frequency with average rocket combustion-chamber pressure (throttling). Rocket chamber characteristic length, 200 inches.

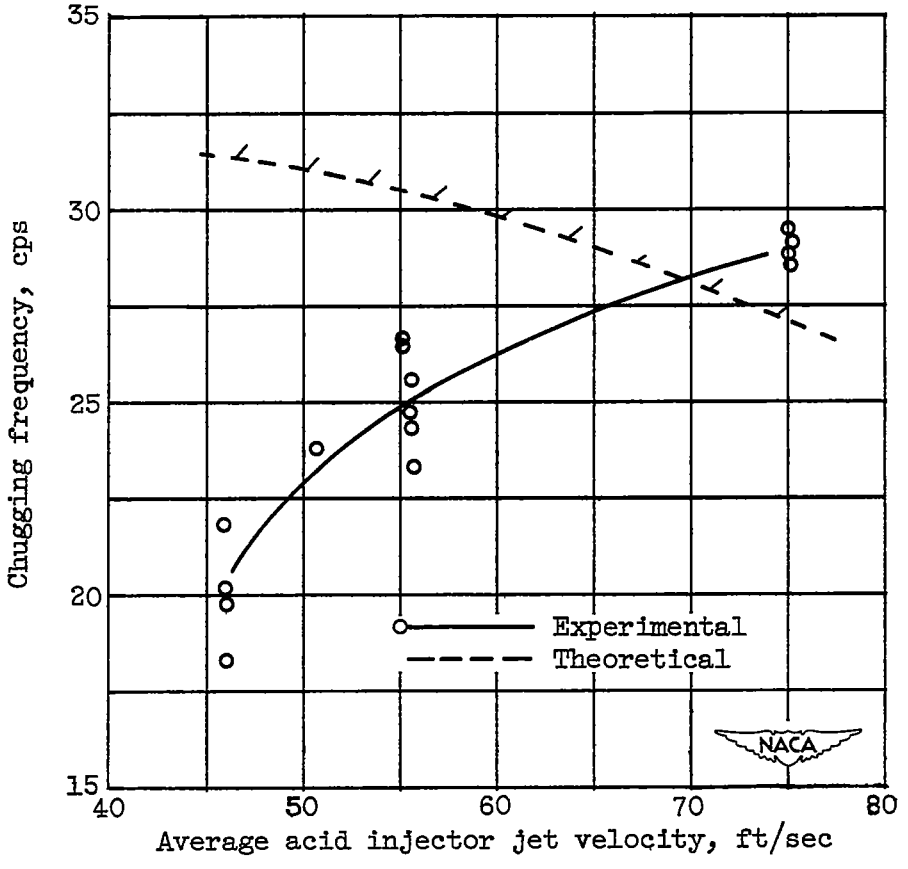

Figure 8. - Experimental variation of chugging frequency with average acid injection stream velocity. Rocket chamber characteristic length, 200 inches; average chamber pressure, 280 pounds per square inch absolute.

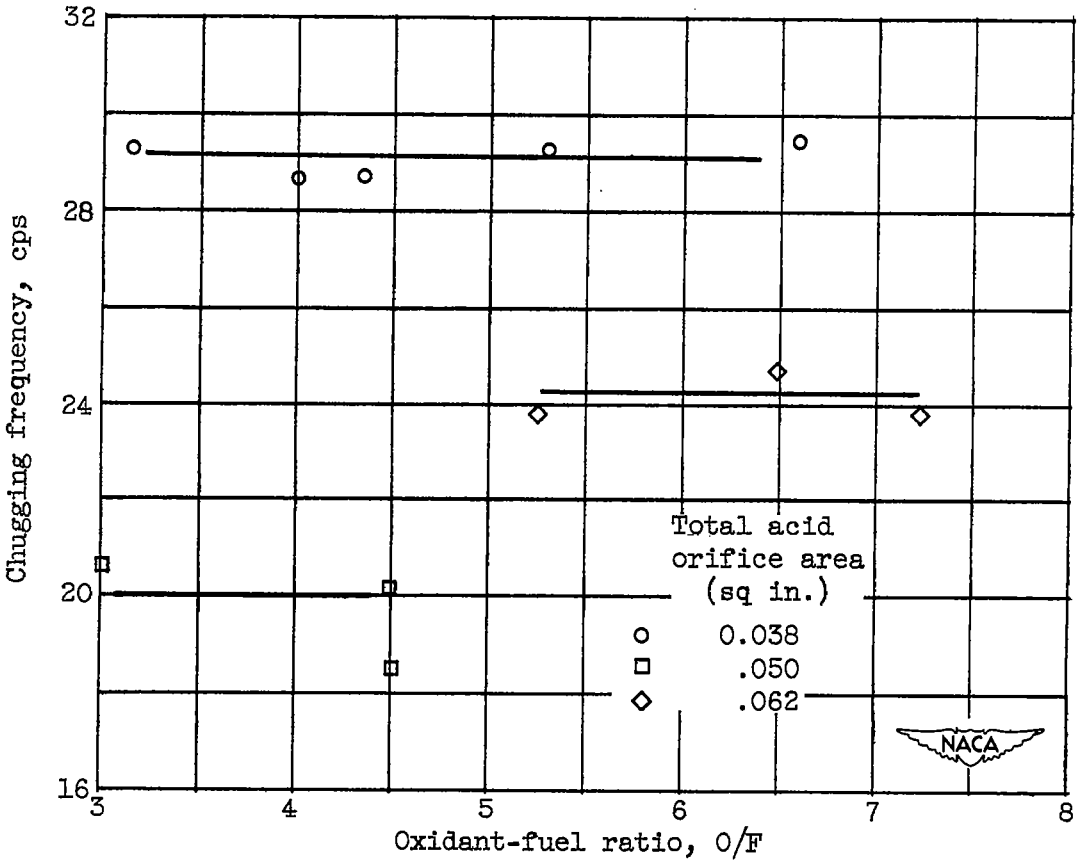

Figure 9. - Experimental variation of chugging frequency with oxidant-fuel ratio. Rocket chamber characteristic length, 200 inches; average chamber pressure, 280 pounds per square inch absolute.

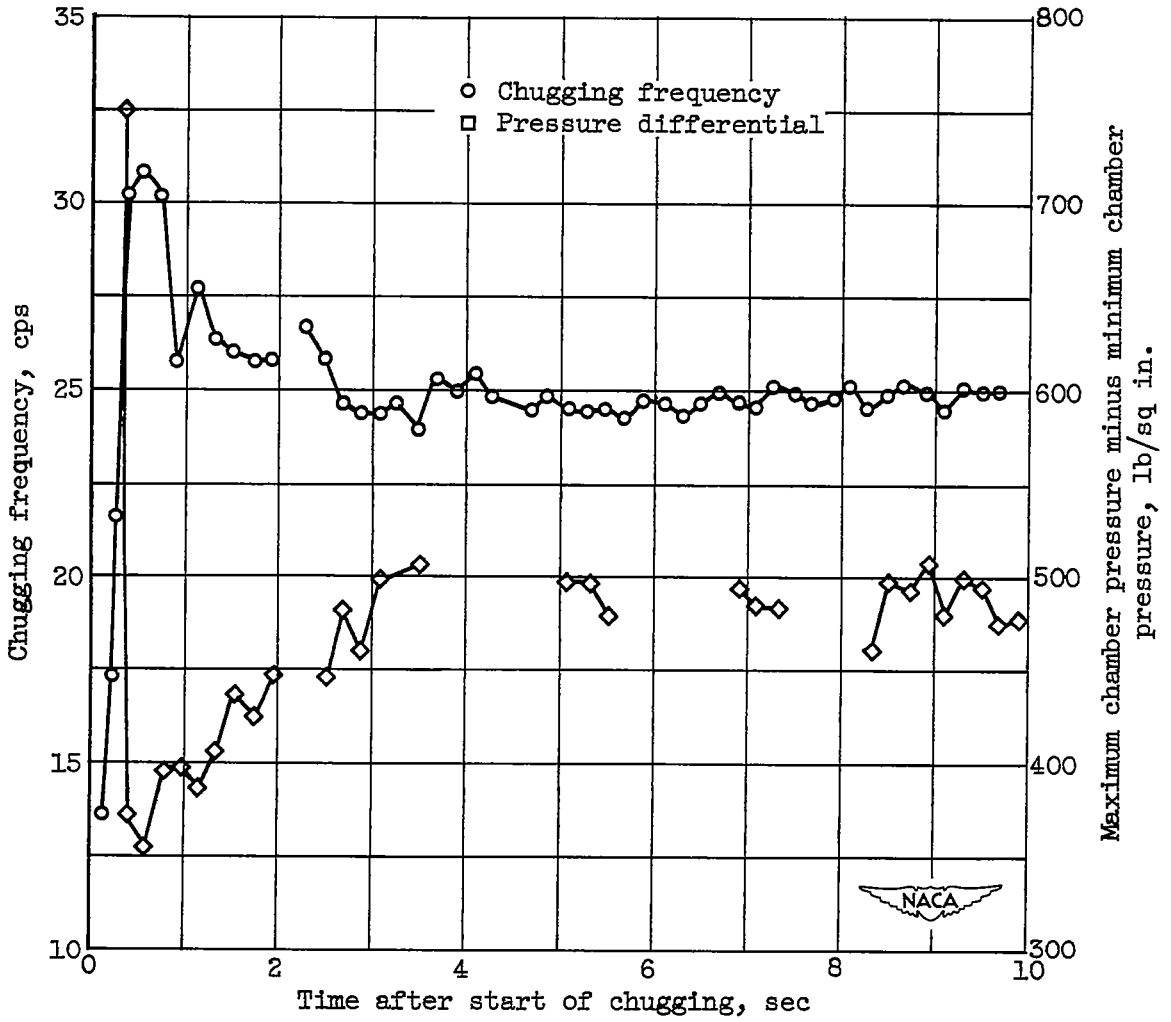

Figure 10. - Experimental variation of chugging frequency and amplitude of chamber pressure fluctuations with time after start of chugging. Rocket chamber characteristic length, 200 inches; average chamber pressure, 270 pounds per square inch absolute.

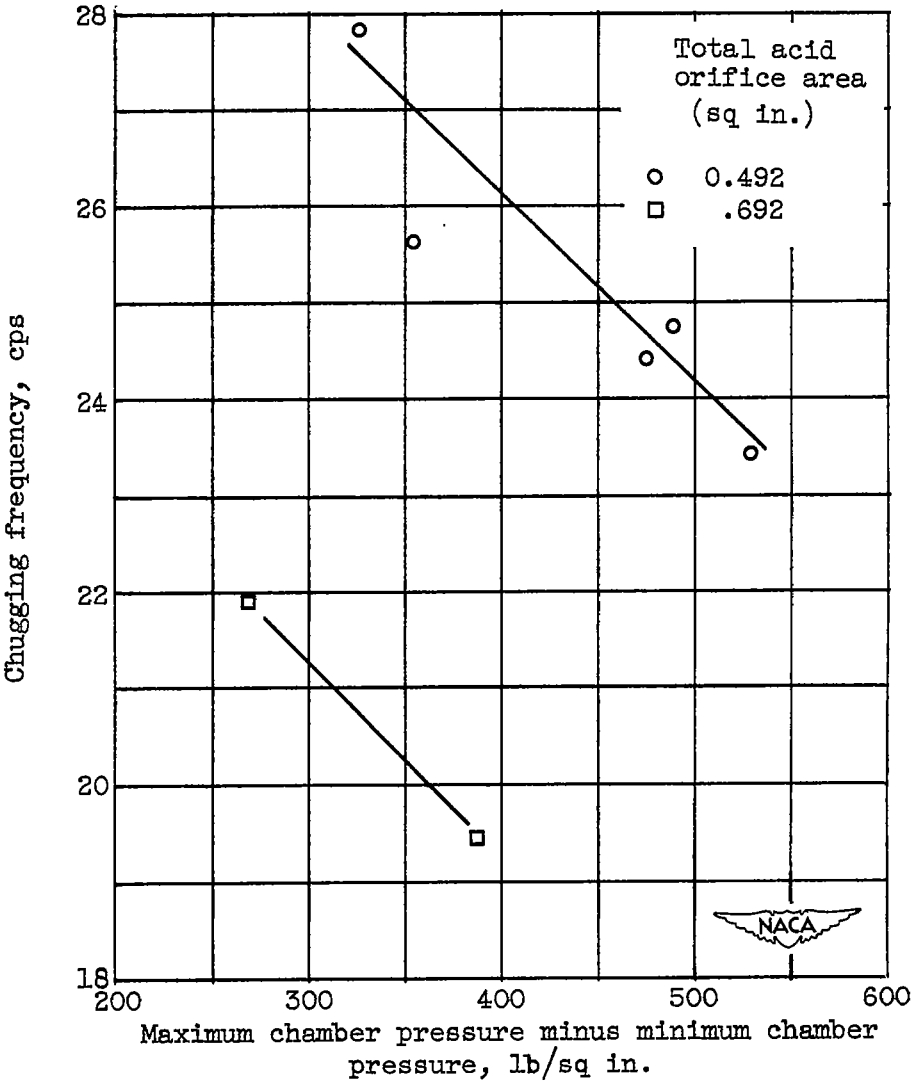

Figure 11. - Experimental variation of chugging frequency with amplitude of chamber pressure fluctuations. Rocket chamber characteristic length, 200 inches; average chamber pressure, 270 pounds per square inch absolute.

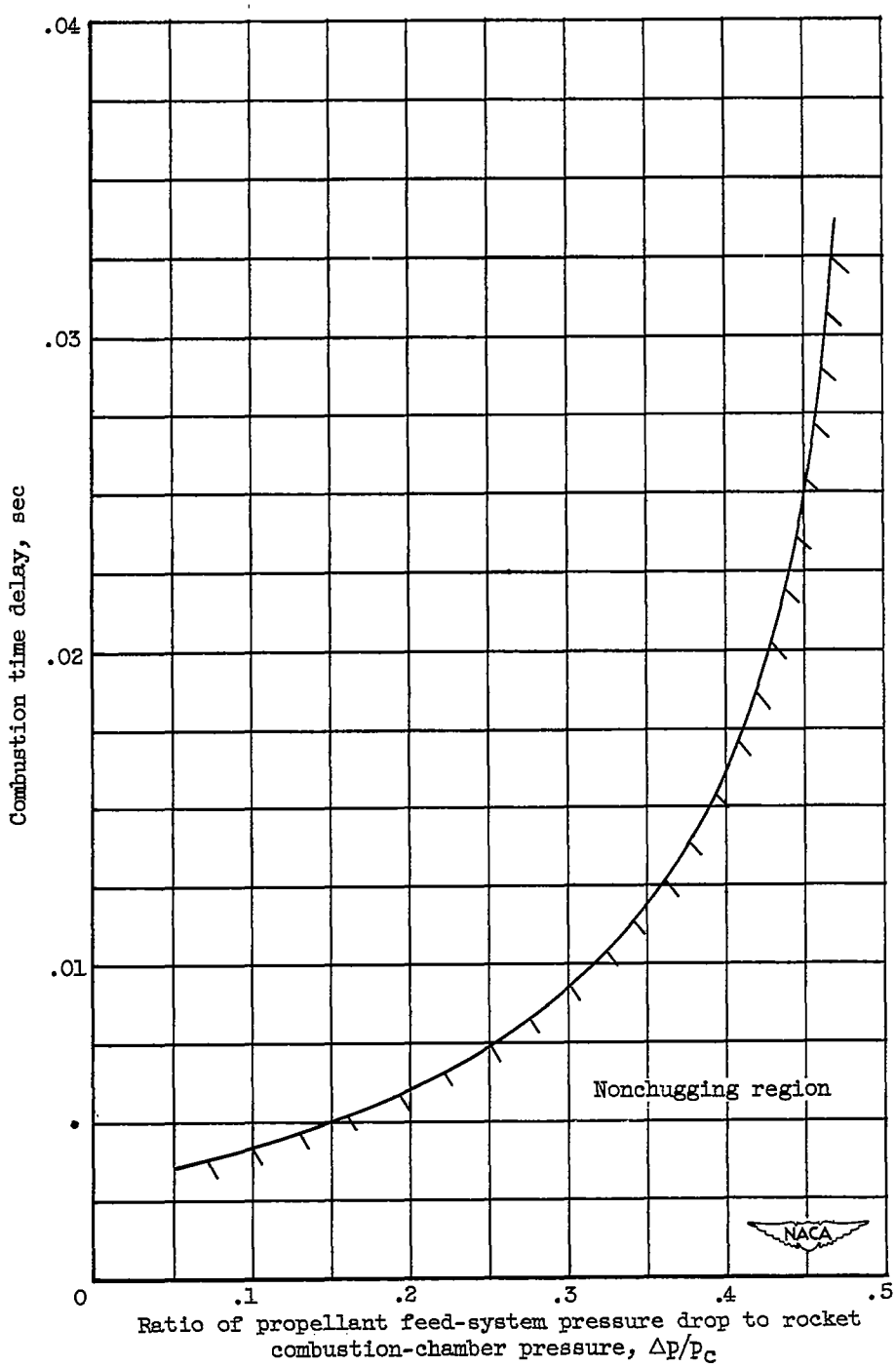

Figure 12. - Variation of combustion time delay with ratio of propellant feed-system pressure drop to rocket combustion-chamber pressure. Rocket chamber characteristic length, 100 inches; combustion-chamber pressure, 300 pounds per square inch absolute; length of propellant feed line, 4 feet; cross-sectional area of propellant feed line, 0.2485 square inch; rocket engine thrust, 300 pounds; specific impulse, 187.5 pound-seconds per pound.

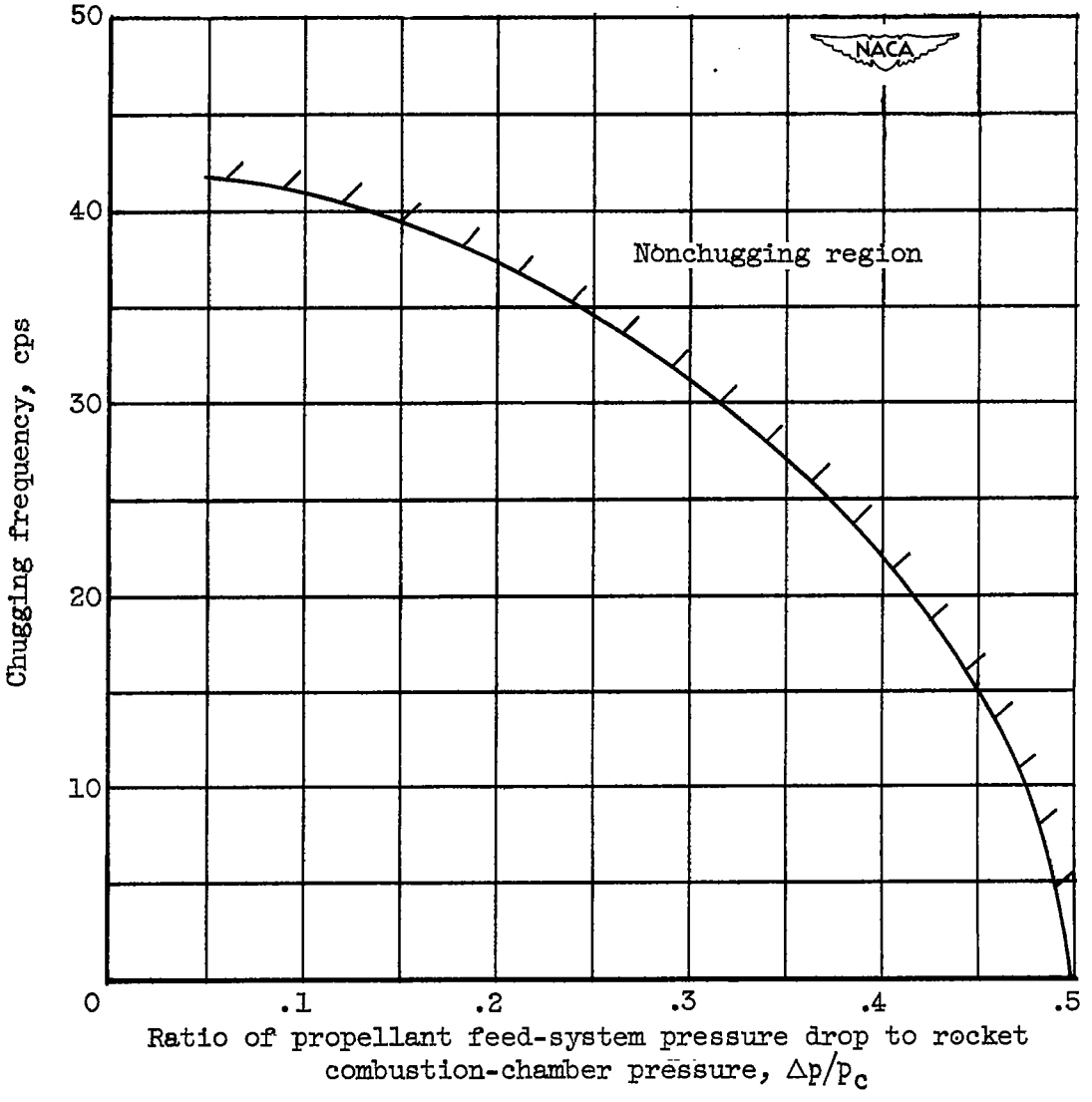

Figure 13. - Variation of chugging frequency with ratio of propellant feed-system pressure drop to rocket combustion-chamber pressure. Rocket chamber characteristic length, 100 inches; combustion-chamber pressure, 300 pounds per square inch absolute; length of propellant feed line, 4 feet; cross-sectional area of propellant feed line, 0.2485 square inch; rocket engine thrust, 300 pounds; specific impulse, 187.5 pound-seconds per pound.

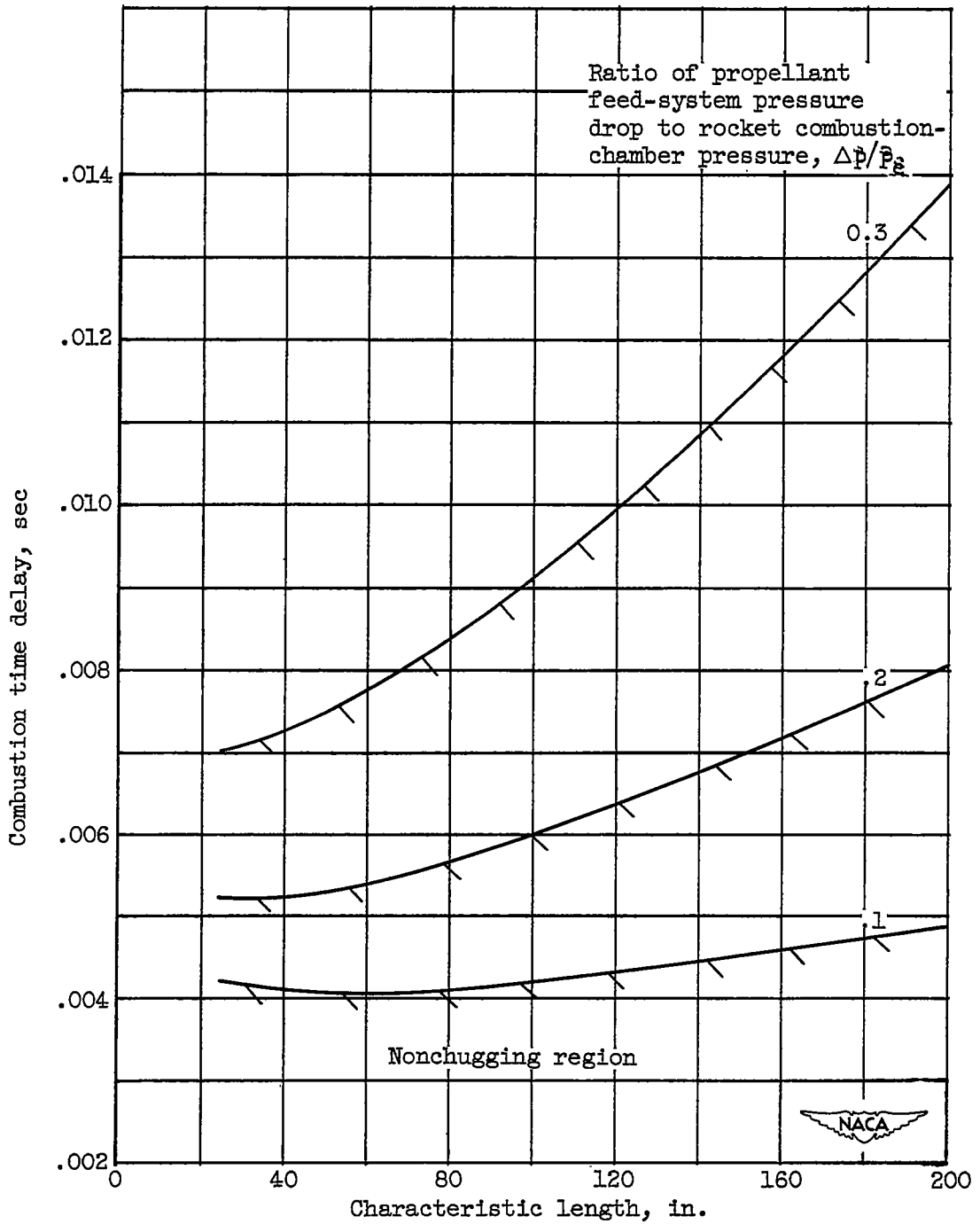

Figure 14. - Variation of combustion time delay with rocket combustion-chamber characteristic length. Combustion-chamber pressure, 300 pounds per square inch absolute; length of propellant feed line, 4 feet; cross-sectional area of propellant feed line, 0.2485 square inch; rocket engine thrust, 300 pounds; specific impulse, 187.5 pound-seconds per pound.

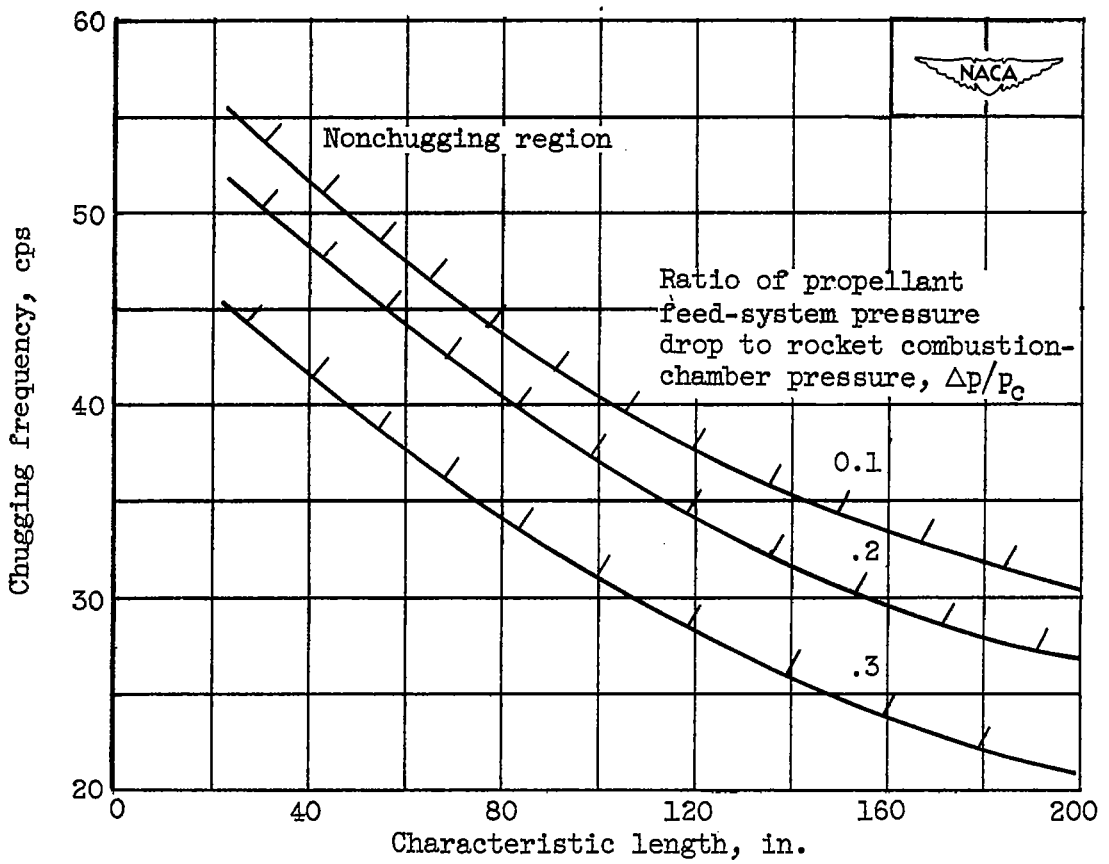

Figure 15. - Variation of chugging frequency with rocket combustion-chamber characteristic length. Combustion-chamber pressure, 300 pounds per square inch absolute; length of propellant feed line, 4 feet; cross-sectional area of propellant feed line, 0.2485 square inch; rocket engine thrust, 300 pounds; specific impulse, 187.5 pound-seconds per pound.

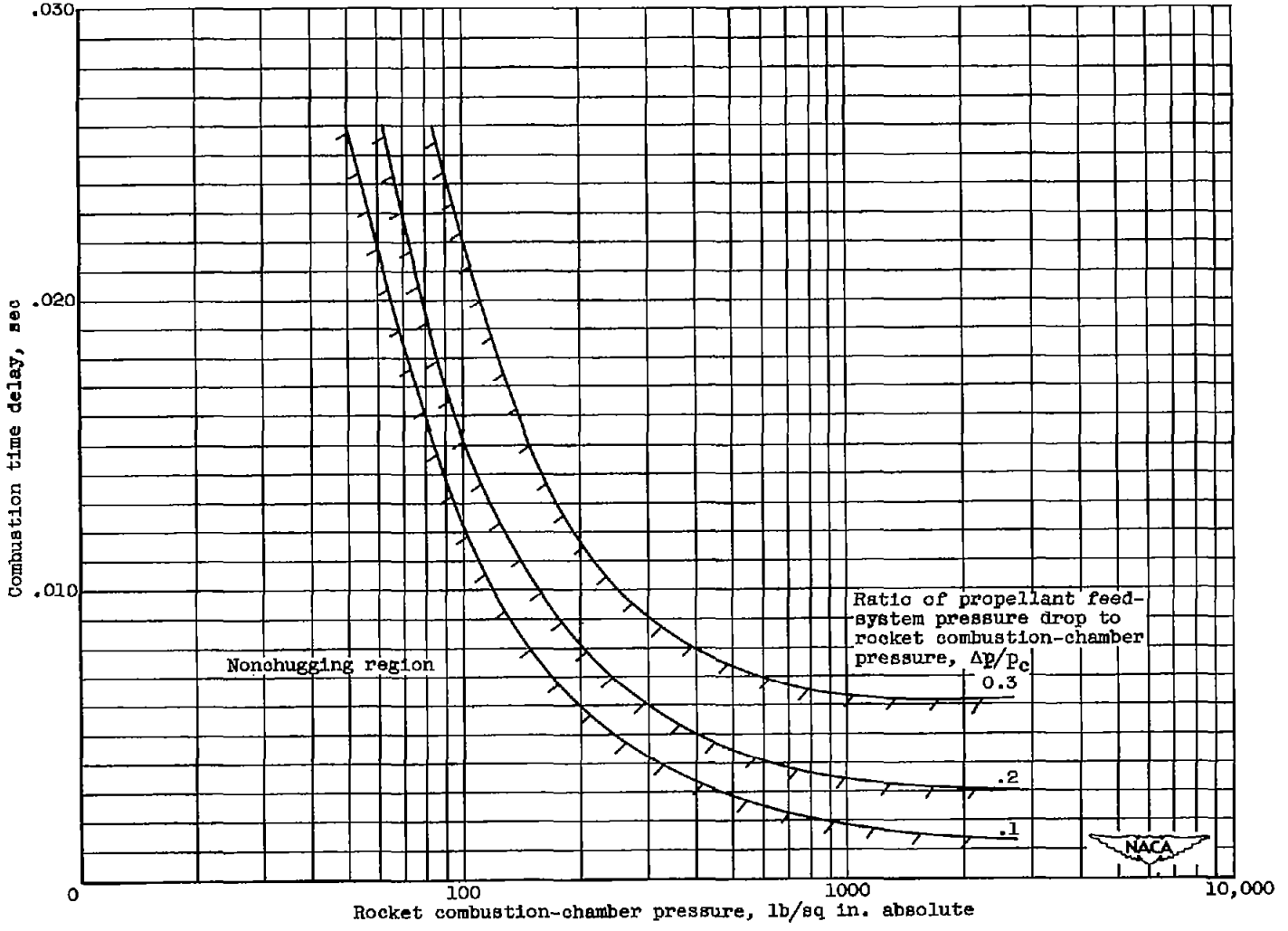

Figure 16. - Variation of combustion time delay with rocket combustion-chamber pressure. Rocket chamber characteristic length, 100 inches; length of propellant feed line, 4 feet; area of propellant feed line, 0.2485 square inch; rocket engine thrust, 300 pounds; specific impulse, 187.5 pound-seconds per pound.

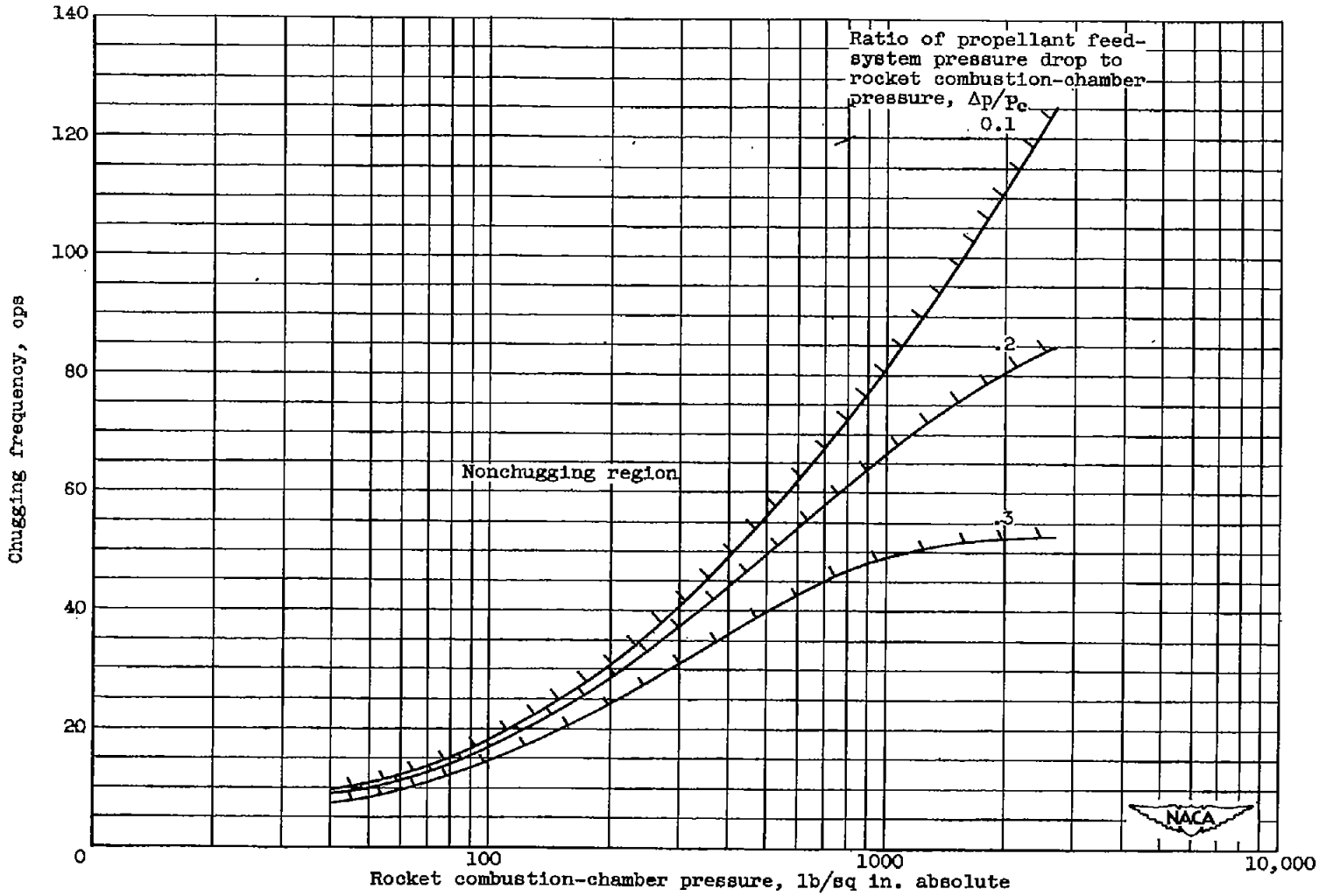

Figure 17. - Variation of chugging frequency with rocket combustion-chamber pressure. Rocket chamber characteristic length, 100 inches; length of propellant feed line, 4 feet; area of propellant feed line, 0.2485 square inch; rocket engine thrust, 300 pounds; specific impulse, 187.5 pound-seconds per pound.

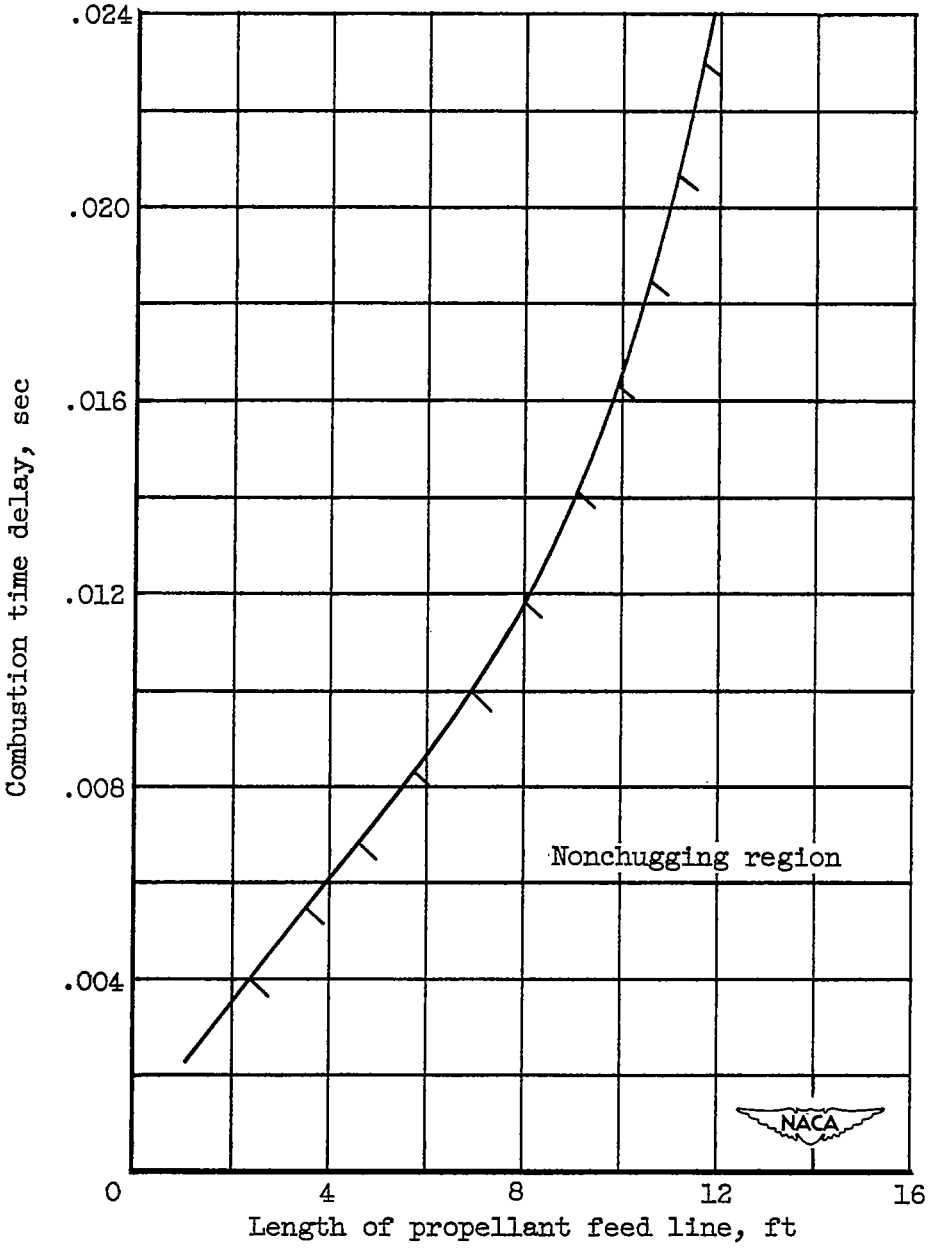

Figure 18. - Variation of combustion time delay with length of propellant feed line. Rocket chamber characteristic length, 100 inches; combustion-chamber pressure, 300 pounds per square inch absolute; area of propellant feed line, 0.2485 square inch; rocket engine thrust, 300 pounds; specific impulse, 187.5 pound-seconds per pound.

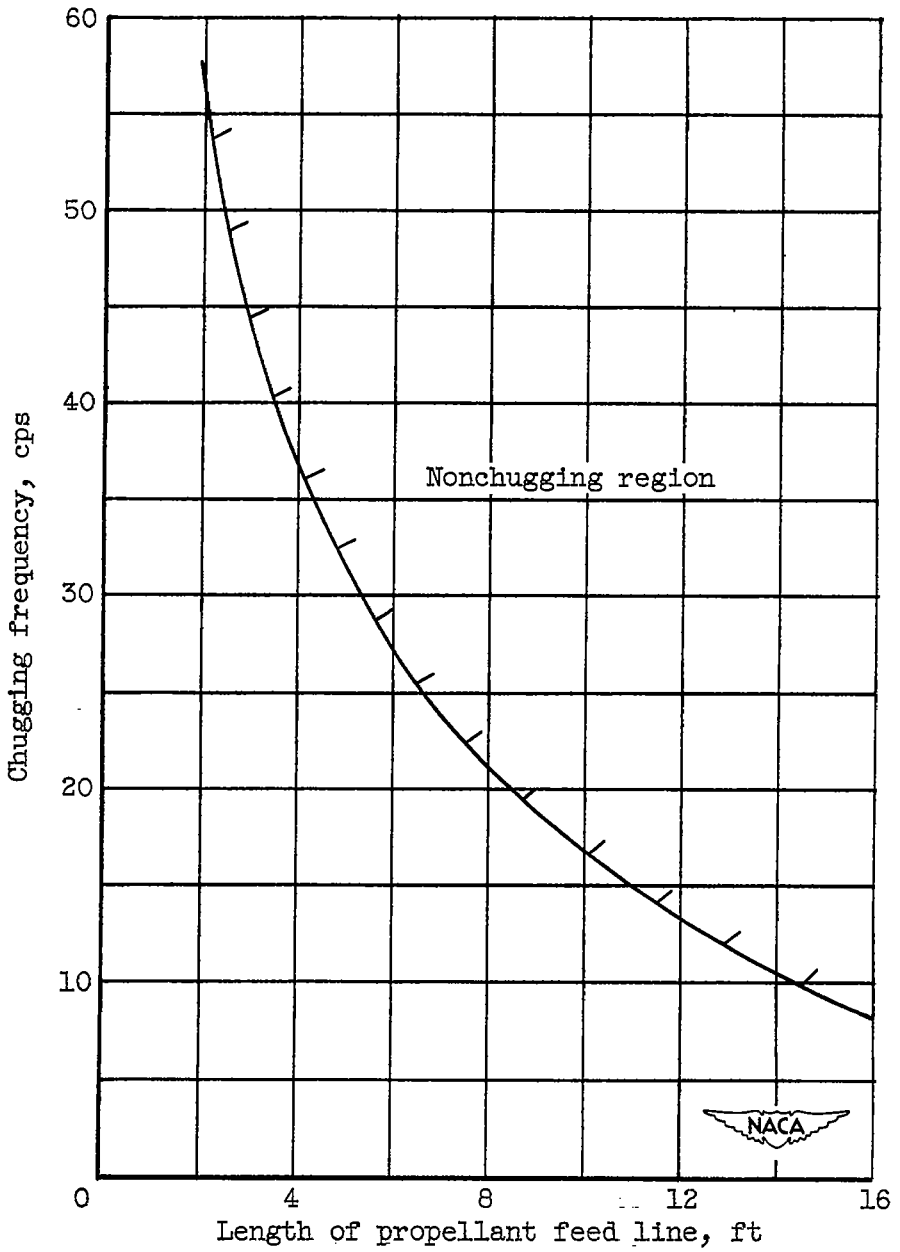

Figure 19. - Variation of chugging frequency with length of propellant feed line. Rocket chamber characteristic length, 100 inches; combustion-chamber pressure, 300 pounds per square inch absolute; area of propellant feed line, 0.2485 square inch; rocket engine thrust, 300 pounds; specific impulse, 187.5 pound-seconds per pound.

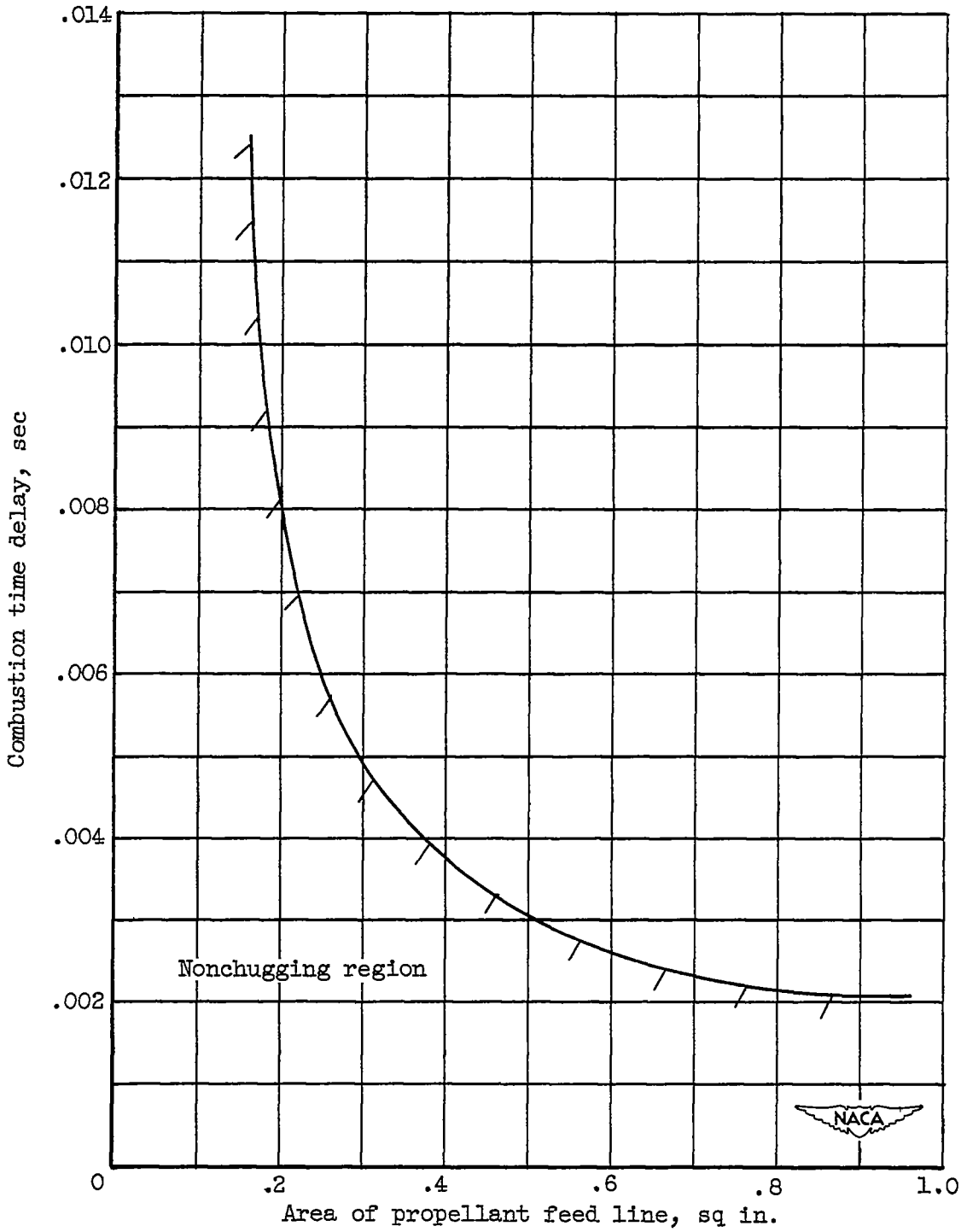

Figure 20. - Variation of combustion time delay with propellant line area. Rocket chamber characteristic length, 100 inches; combustion-chamber pressure, 300 pounds per square inch absolute; length of propellant feed line, 4 feet; rocket engine thrust, 300 pounds; specific impulse, 187.5 pound-seconds per pound.

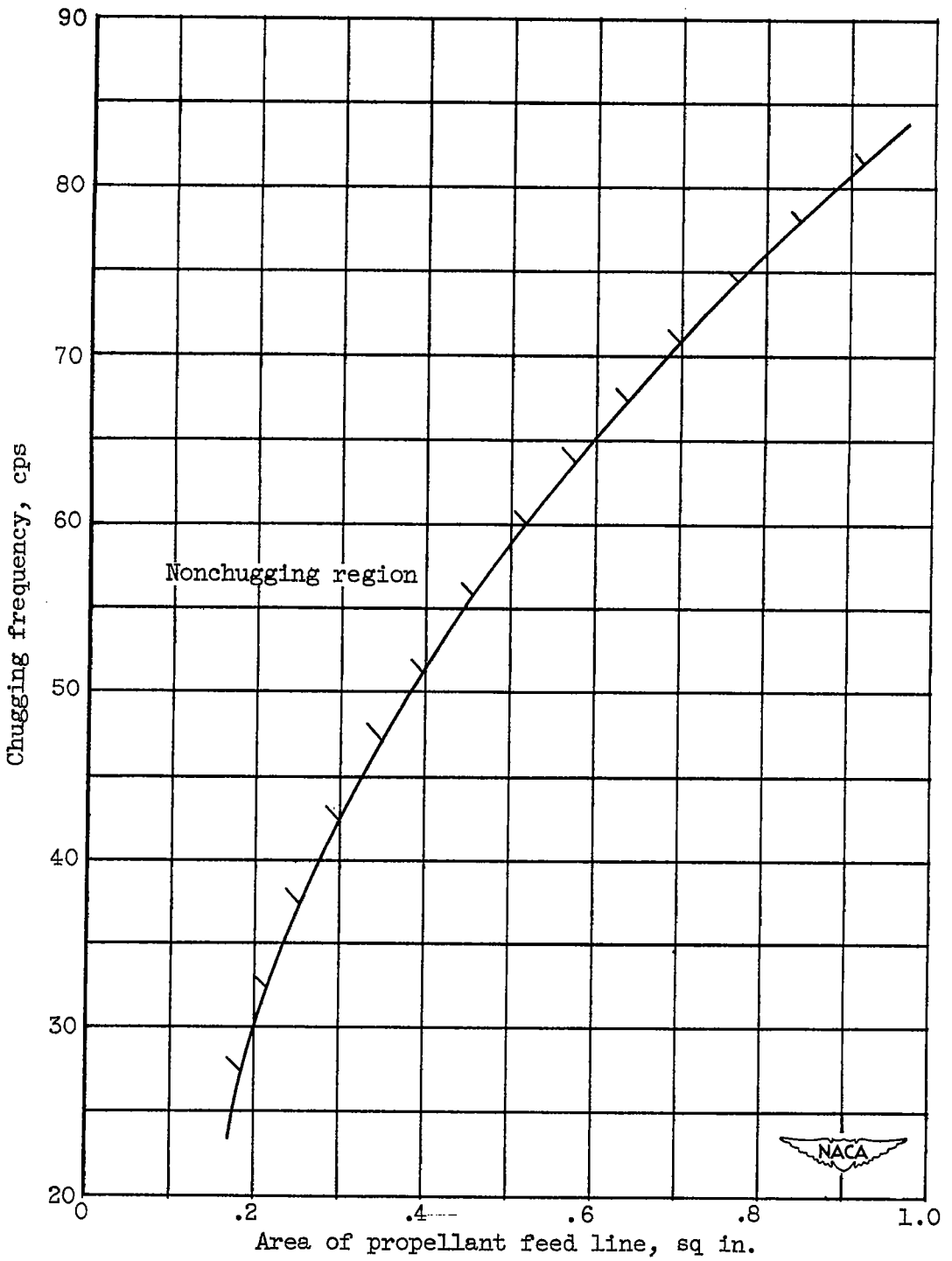

Figure 21. - Variation of chugging frequency with propellant line area. Rocket chamber characteristic length, 100 inches; combustion-chamber pressure, 300 pounds per square inch absolute; length of propellant feed line, 4 feet; rocket engine thrust, 300 pounds; specific impulse, 187.5 pound-seconds per pound.